INTERNATIONAL STUDIES IN THE FIELD OF

MECHANICAL ENGINEERING

EDITOR

Doç. Dr. Nurullah GÜLTEKİN

DECEMBER 2025

gece kitaplığı

İmtiyaz Sahibi / Yaşar Hız
Yayına Hazırlayan / Gece Kitaplığı

Birinci Basım / Aralık 2025 - Ankara
ISBN / 978-625-8570-59-5

© copyright
Bu kitabın tüm yayın hakları Gece Kitaplığı'na aittir.
Kaynak gösterilmeden alıntı yapılamaz, izin almadan hiçbir yolla çoğaltılamaz.

Gece Kitaplığı
Kızılay Mah. Fevzi Çakmak 1. Sokak
Ümit Apt No: 22/A Çankaya/ANKARA
0312 384 80 40
www.gecekitapligi.com / gecekitapligi@gmail.com

Baskı & Cilt
Bizim Büro
Sertifika No: 42488

INTERNATIONAL STUDIES IN THE FIELD OF MECHANICAL ENGINEERING

ARALIK 2025

EDITOR

Doç. Dr. Nurullah GÜLTEKİN

gece kitaplığı

CONTENTS

CHAPTER 1

THE ROLE OF BINDERS IN PELLET BIOFUEL PRODUCTION AND THEIR EFFECTS ON PELLET QUALITY

Bekir DOĞAN[1], Ünsal AYBEK[2]

1 Asst. Prof. Dr. Tokat Gaziosmanpasa University, Tokat Vocational School, Department of Machine and Metal Technologies, Orcid: 0000-0002-8986-7174
2 Asst. Prof. Dr. Tokat Gaziosmanpasa University, Tokat Vocational School, Department of Electricity and Energy, Orcid: 0000-0003-3573-9385

1.Introductıon

Biomass-based solid biofuels play a key role in sustainable energy systems due to their low carbon footprint, regional availability, and contributions to energy security (Jordan et al., 2019). Among these fuels, biomass pellets have gained widespread acceptance owing to their high bulk density, low moisture content, uniform combustion behavior, and compatibility with automated heating systems (Goh et al., 2013).

Maintaining high pellet quality requires not only suitable feedstock properties but also the optimization of pelletization parameters, including moisture, temperature, pressure, and binder utilization. Insufficient particle adhesion during densification often leads to low mechanical durability, excessive fines, reduced density, and operational problems in pellet mills (Stelte et al., 2011). These challenges are more prominent in low-lignin agricultural residues, fibrous materials with weak inter-particle bonding, and biomass with high inorganic content, where natural binding mechanisms are inadequate (Samuelsson et al., 2012).

Therefore, the application of binders has become an essential strategy for producing durable and standardized pellets, particularly from low-quality or heterogeneous biomass sources. Binders enhance particle adhesion during densification, reduce energy consumption in pellet mills, and significantly improve pellet density, abrasion resistance, hygroscopic behavior, and combustion performance (Tumuluru, 2014). However, binder selection must be carried out carefully, as certain binders can influence ash content, slagging tendencies, and gaseous emissions either positively or negatively (García-Maraver et al., 2011).

This chapter provides a comprehensive overview of the mechanisms, classifications, and quality impacts of binders in pellet biofuel production. Additionally, commonly used binder types from the literature are summarized, and the potential of cotton dust as a natural fiber-based binder is evaluated as an example of an innovative and cost-effective additive.

2.Fundamental Properties of Binders

Binders in pellet biofuel production are additives that enhance adhesion and cohesion among biomass particles during densification, thereby improving mechanical durability, density, and overall pellet quality. Their effectiveness depends on multiple factors including feedstock characteristics, chemical composition, moisture content, and pelletization parameters (Ungureanu et al., 2018).

Binders function by reinforcing the physical, thermal, and chemical interactions among biomass particles under high pressure and temperature. The success of binder action is strongly related to the formation of inter-particle bonding bridges, which provide structural integrity to the pellet (Anukam et al., 2021).

2.1 What is a Binder?

A binder is defined as an organic or inorganic substance that facilitates particle adhesion, improves plasticity during pelletization, and forms a stable structural matrix upon cooling. Binders serve three primary functions:

- Adhesion — interaction between binder and particle surfaces.
- Cohesion — internal bonding within the binder matrix.
- Bridge Formation — solid or semi-solid connections formed during drying or cooling.

The performance of a binder is directly linked to its ability to create stable micro- and macro-level bonding networks within the pellet structure.

2.2 Binder Mechanisms

The mechanisms through which binders enhance pellet structure can be categorized into four primary pathways:

a) Lignin Softening and Thermal Interactions

Natural lignin softens between 140–180 °C and acts as an intrinsic binder. Low-lignin biomass requires external binders to compensate for this deficiency (Lizundia et al., 2021).

b) Physical Bonding and Fiber Interlocking

Fiber-rich binders such as cotton dust or straw fines promote mechanical interlocking between particles (Stelte et al., 2011).

c) Gelatinization and Chemical Bonding

Starch-based binders undergo gelatinization during heating, producing a strong adhesive matrix (Ahn et al., 2014).

d) Capillary Forces and Moisture-Induced Adhesion

Capillary bridges formed by moisture during compression support temporary adhesion, contributing to initial pellet shape formation before solidification (Kaliyan & Morey, 2010). Together, these mechanisms enhance pellet durability, density, and overall structural stability.

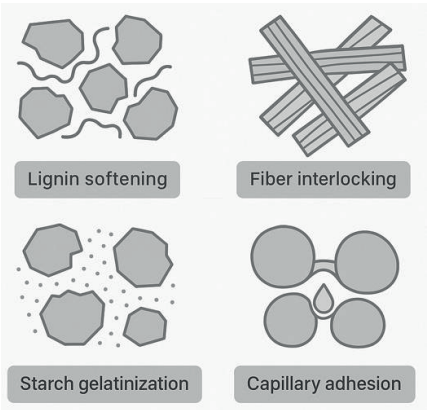

Figure 2.1. Mechanisms of Binder Action in Biomass Pelletization

3. Types of Binders

Binders used in pellet biofuel production can be categorized based on their origin, chemical structure, and bonding mechanisms. (Butler et al., 2023). The primary groups include natural binders**,** industrial/organic binders**,** and agricultural waste-derived binders**.**

Table 3.1. Comparison of Major Binder Types Used in Biomass Pelletization

Binder Type	Source / Origin	Primary Mechanism	Advantages	Limitations	Typical Dosage
Starch	Corn, wheat, potato	Gelatinization → strong adhesive matrix	High durability ↑, good cohesion	Hygroscopicity ↑, risk of microbial growth	1–5%
Lignosulfonates	Pulping industry by-product	Chemical bonding via sulfonate groups	Durability ↑↑, density ↑, lubrication effect	Ash ↑ slightly, dark color	0.5–2%
Glycerol / Crude Glycerin	Biodiesel production	Plasticization, lubrication	Energy consumption ↓, flowability ↑	Excess softening at high ratios	1–3%
Molasses	Sugar processing residue	Sugar caramelization → coating	Durability ↑, fines ↓	CO emissions ↑, sticky handling	2–5%
Fiber-rich Additives (cotton dust, straw fines)	Agricultural residues	Mechanical interlocking	Low ash, low cost, improved structure	Low chemical bonding, needs blending	5–20%
Bio-oils / Pyrolytic Lignin	Pyrolysis & HTL products	Aromatic polymerization	Strong bonding, hydrophobicity ↑	Odor, variable viscosity	1–4%
Inorganic Binders (clays, bentonite)	Natural minerals	Filling & bridging	Improved shape stability	Ash ↑↑, HHV ↓	0.5–2%

3.1 Natural Binders

These are widely used due to their biodegradability, low cost, and compatibility with biomass.

a) Starch (corn, wheat, potato starch)

- Undergoes gelatinization upon heating, forming a continuous adhesive matrix between biomass particles. (Ståhl et al., 2012; Hu et al., 2015)
- Provides strong adhesive properties even at low dosages (typically <2 wt%), increasing pellet hardness and reducing abrasion and fines (Butler et al., 2023; Ahn et al., 2014).
- At higher proportions it can increase hygroscopicity and equilibrium moisture content of the pellets, which may affect storage stability (Wang et al., 2020; Anukam et al., 2021).

b) Lignosulfonates

Lignosulfonates are among the most effective and widely used natural binders in biomass pelletization. They are generated as by-products of the sulfite pulping process and contain sulfonate functional groups that enable strong chemical bonding with biomass components.

Key mechanisms include:

- Formation of cross-linking bridges between cellulose, hemicellulose, and lignin fragments
- Improved die lubrication due to their surfactant-like behavior
- Enhanced thermal softening**,** promoting compact and dense pellet structures

Numerous studies have shown that lignosulfonates significantly increase pellet mechanical durability (up to 20–40%), reduce fines generation, and enhance bulk density, even at low addition levels (typically0.5–2wt%) (Nielsen et al., 2009; Kaliyan & Morey, 2010; Tumuluru, 2014).

These properties make lignosulfonates one of the most powerful and industrially preferred organic binders in pellet production.

c) Molasses

Molasses is a viscous by-product of sugar refining and contains high concentrations of sucrose, glucose, fructose, and various organic compounds. Due to its sticky, hygroscopic, and film-forming nature, molasses acts as an effective natural binder during pelletization.

During pressing, molasses spreads as a viscous coating layer around biomass particles, increasing cohesion and reducing fines.
It also contributes to thermal softening, which improves densification behavior.

However, at high proportions, molasses may increase moisture uptake and can lead to slightly higher CO emissions during combustion due to its sugar content (Kaliyan & Morey, 2010; Adapa et al., 2009; Oladeji, 2010).

d) Vegetable Oils

Vegetable oils (such as soybean, rapeseed, linseed, and sunflower oil) are commonly used as lubricating additives in pelletization. Because of their low viscosity and hydrophobic molecular structure, they effectively reduce friction inside the die, lowering required compression energy and preventing die overheating.

However, their direct impact on mechanical durability is generally limited. Vegetable oils do not form strong chemical or solid bridges between biomass particles; instead, they primarily improve pelletization efficiency by enhancing lubrication and flowability of the material.

At excessive dosages, vegetable oils may even reduce pellet durability due to over-lubrication, leading to insufficient inter-particle bonding and weaker structural compaction (Stelte et al., 2011; Tumuluru, 2014).

3.2 Industrial and Organic Binders

These binders originate from industrial residues and often possess strong adhesion properties.

a) Glycerol and Crude Glycerin

Glycerol and crude glycerin—major by-products of biodiesel production—are widely used as organic binders and plasticizing agents in biomass pelletization. Due to their hydroxyl-rich molecular structure, they reduce the glass transition temperature of biomass polymers, improving plasticity and deformability under compression.

Their lubricating behavior decreases internal die friction, which:

- lowers energy consumption during densification,
- improves feedstock flowability,
- reduces die wear,
- and stabilizes pellet production rates.

However, excessive addition of glycerol can soften pellets and reduce durability, as it does not create strong solid bridges between particles. Optimal dosages reported in literature are generally within 1–5 wt%**,** depending on biomass type and moisture content (Emami et al., 2015; Tumuluru, 2014; Strezov et al., 2019).

b) Pyrolytic Lignin and Bio-oils

Pyrolytic lignin and bio-oils are liquid by-products generated during fast pyrolysis and hydrothermal liquefaction (HTL) of lignocellulosic biomass.

Their high content of aromatic phenolic compounds, lignin fragments, and oxygenated polymers provides strong adhesive properties during pelletization.

Due to their thermoplastic behavior, these liquids:

- promote softening and fusion of biomass particles,
- form polymeric adhesive films upon cooling,
- enhance inter-particle bonding**,**
- and can increase pellet density and durability at low addition rates (1–5 wt%).

However, high dosages may increase moisture, reduce stability, or cause odor/darkening in pellets.

Their variable composition (depending on pyrolysis temperature and feedstock) also requires careful optimization (Hu et al., 2015).

c) Paper Mill Sludge

Paper mill sludge, generated from pulp and paper manufacturing, is a fiber-rich residue containing significant amounts of cellulose, hemicellulose, and mineral fillers. Owing to its

fibrous morphology and high surface area, it promotes mechanical interlocking between biomass particles during pelletization.

The presence of short cellulose fibers enhances inter-particle bonding**,** increases pellet density, and reduces fines formation. Additionally, its moderate moisture content can aid compressibility; however, high ash content (originating from fillers like kaolin and calcium carbonate) may limit its use in premium pellet grades (e.g., ENplus A1).

Optimal addition levels typically range from 5–20 wt%**,** depending on sludge composition, initial moisture, and biomass type (Matúš et al., 2018).

3.3 Agricultural and Waste-Derived Binders

These binders are sustainable, low-cost, and increasingly preferred.

a) Cotton Dust

Cotton dust, generated during cotton ginning, carding, and spinning operations, is a fine fibrous residue composed primarily of cellulose-rich short fibers**,** lint fragments**,** and minute plant particles**.**
Its fibrous morphology provides excellent mechanical fiber interlocking**,** which enhances pellet cohesion and structural stability during densification.

Because cotton dust contains very low ash (typically 0.5–1.5 wt%**),** it does not significantly increase the ash content of pellets—an important advantage for meeting premium fuel standards (e.g., ENplus A1/A2).

Its high availability in textile and ginning industries, combined with its low cost, makes cotton dust an attractive binder or co-fiber additive in biomass pelletization.

Cotton dust addition (typically 5–20 wt%**)** improves durability, reduces fines, and enhances packing density, especially when mixed with low-lignin agricultural residues. (Suvunnapob et al., 2015; Espinoza-Tellez et al., 2020).

b) Wheat Straw Fines

Wheat straw fines, generated during milling, chopping, and grinding operations, consist predominantly of cellulose and hemicellulose fibers with relatively low lignin content (typically 12–16%).
Their fibrous structure promotes mechanical interlocking during pelletization, improving particle cohesion and reducing fines formation.

However, due to the low lignin content, wheat straw fines exhibit limited thermoplastic behavior, resulting in weaker chemical bonding compared to woody biomass. This often leads to lower durability and higher abrasion unless binders or pre-treatments (e.g., steam explosion, torrefaction, moisture optimization) are applied.

Despite these limitations, wheat-straw-derived fines remain widely used as a low-cost, renewable additive or co-biomass in pellet formulations, particularly when combined with higher-lignin materials (Kaliyan & Morey, 2010; Serrano et al., 2011; Samuelsson et al. 2012).

c) Olive Pomace and Kernel Powder

Olive pomace and olive kernel powder are by-products generated during olive oil extraction processes (two-phase or three-phase systems). These residues contain cellulose, hemicellulose, residual lignin, waxes, and olive oil traces, giving them moderate binding capability during pelletization.

Their fine particle structure and partial oil content enhance plastic deformation and offer limited adhesion, improving densification to some extent. However, the ash content of olive pomace is typically higher (3–7%) due to the presence of soil particles, mineral residues, and fruit skin fragments.
This elevated ash restricts its use in premium pellet classes (e.g., ENplus A1) unless blended with low-ash biomass.

Olive kernel powder generally contains more lignin compared to the pomace fraction and may contribute better mechanical stability, but both materials benefit from blending with wood or other low-ash feedstocks to achieve acceptable durability and emission properties (Christoforou & Fokaides, 2016; García Martín et al., 2020).

d) Rice Husk, Corn Stover, and Other Agricultural Particles

Rice husk, corn stover, and similar agricultural residues represent some of the most abundant lignocellulosic materials available globally. These particles are composed mainly of cellulose, hemicellulose, and variable amounts of lignin, ash, and silica**,** depending on the residue type.

Their fibrous structure offers structural reinforcement during pelletization through mechanical interlocking. Rice husk and corn stover fines can improve particle packing and stabilise densification when blended with woody biomass or other high-lignin feedstocks.

However, rice husk contains high silica (15–20%)**,** which contributes to elevated ash levels and abrasion during combustion or pellet milling equipment wear.

Corn stover provides better compaction and moderately higher lignin than rice husk, improving durability compared with other low-lignin agricultural residues.

These residues are low-cost, renewable, and widely available**,** making them attractive co-biomass additives for pellet production, especially in regions with large cereal production systems (Kaliyan & Morey, 2010; Sam Obu et al., 2022; Gilbert et al. 2009).

4. Effects of Binders on Pellet Quality

Binders play a critical role in determining the overall quality of biomass pellets by influencing their physical**,** mechanical**,** thermal**,** chemical**,** and process-related characteristics. Their mode of action depends on the binder's chemical composition, thermal behavior, dosage, and interaction with the biomass matrix. Proper binder selection becomes especially important when working with low-lignin**,** high-ash, or poorly compressible feedstocks, where natural binding mechanisms are insufficient.

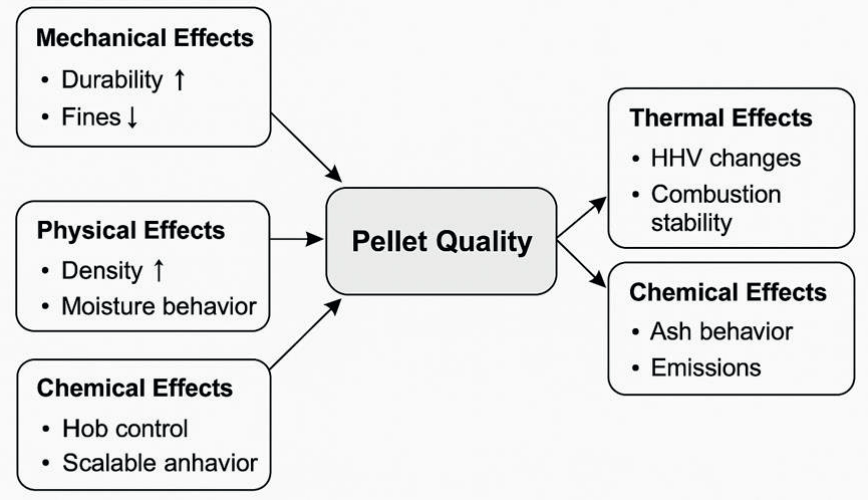

Figure 4.1. Effects of Binders on Pellet Quality

Binders can improve pellet quality through several pathways:

- Physical effects: enhancement of particle packing, reduction of fines, and stabilization of pellet structure.
- Mechanical effects: increased tensile strength, higher durability, improved abrasion resistance, and reduced breakage during handling.
- Thermal effects: facilitation of softening during compression (e.g., lignin activation, plasticization), improving energy efficiency.
- Chemical effects: formation of solid bridges, polymeric films, hydrogen bonding, or chemical cross-linking between biomass components.
- Process effects: reduced die friction, decreased energy consumption, improved throughput, and stabilization of pellet dimensions.

These improvements are well-documented in the literature. Stelte et al. (2011) describe the fundamental bonding mechanisms of biomass densification—including solid bridging, mechanical interlocking, and film formation—while Tumuluru (2014) identifies how additives modify feedstock flowability, compaction energy, and inter-particle bonding. Together, these studies emphasize that appropriate binder selection enhances pellet performance and can compensate for inherent weaknesses in low-quality agricultural residues**.**

Table 4.1. Summary of Binders' Effects on Pellet Quality

Binder Type	Durability	Density	Fines / Abrasion	Ash & Emissions	Notes
Starch	↑↑	↑	↓ fines	Hygroscopicity ↑	Strong gelatinization; low dosage effective
Lignosulfonates	↑↑↑	↑↑	↓↓ fines	Slight ash ↑	Best industrial binder; lubricates die
Glycerol / Crude Glycerin	↑ (moderate)	↔ or ↑	↓ abrasion	CO ↑ slight	Over-dosage softens pellets
Molasses	↑	↔	↓ fines	CO ↑↑	Film-forming; sticky handling
Fiber-rich Additives (cotton dust, straw fines)	↑	↔	↓ fines	Ash stable	High mechanical interlocking; low cost
Bio-oils / Pyrolytic lignin	↑↑	↑↑	↓	Dark color, odor ↑	Strong thermoplastic bonding
Inorganic Binders	↑ (shape stability)	↑	↓ fines	Ash ↑↑, HHV ↓	Not suitable for premium pellets

4.1 Physical and Mechanical Effects

a) Mechanical Durability Improvement

Binders play a key role in improving the mechanical durability of biomass pellets, which is critical for minimizing pellet breakage, dust formation, and fines generation during handling, storage, and transportation.

Improved durability enhances fuel logistics and overall pellet performance in industrial applications.

Common binders such as starch, lignosulfonates, and cotton dust enhance durability through different mechanisms:

- Starch increases adhesion via gelatinization, forming a continuous matrix that strengthens particle bonding.
- Lignosulfonates provide strong chemical bonding and solid bridge formation, often producing the highest durability gains.
- Cotton dust**,** due to its fibrous morphology, improves mechanical interlocking and enhances structural integrity.

Experimental studies have shown that these binders can increase pellet durability by approximately 10–40%**,** depending on biomass type, binder dosage, and processing conditions (Nielsen et al., 2009; Ahn et al., 2014; Suvunnapob et al., 2015).

b) Density Enhancement

Binder addition can significantly improve the bulk density and energy density of biomass pellets by enhancing particle packing, reducing void spaces, and promoting more effective compression during densification. Higher density leads to improved handling, reduced transport cost, and greater combustion efficiency.

Two binder groups are especially effective for density enhancement:

- *Lignosulfonates:* Owing to their thermoplastic behavior and chemical bonding capability, lignosulfonates promote particle softening and solid bridge formation. This facilitates tighter compaction and produces pellets with higher unit density.
- *Glycerol / Crude Glycerin:* Glycerol acts as a plasticizer, lowering the glass transition temperature of biomass polymers and improving deformability under pressure. This results in smoother pellet formation and a more homogeneous, dense structure.

Studies have shown that lignosulfonates and glycerol-based binders can increase pellet density by 5–20%**,** depending on biomass type, moisture content, and binder dosage (Emami et al., 2015; Marrugo et al., 2019; Bala-Litwiniak & Radomiak, 2019).

c) Reduction of Fines and Abrasion

Binders play an important role in reducing fines formation and surface abrasion—two key indicators of pellet durability and quality. By enhancing particle bonding and improving

pellet surface integrity, binders minimize the generation of dust during handling, transportation, and storage (Nielsen et al., 2009; Serrano et al., 2011).

Lignosulfonates are particularly effective in fines reduction due to their ability to form solid bridges and polymeric films between particles. Their thermoplastic and adhesive behavior results in smoother pellet surfaces and fewer fractures.

Studies have shown that even low dosages of lignosulfonate (typically 0.5–2 wt%**)** can reduce fines production by 30–50%**,** depending on biomass type and processing conditions. Starch-based binders and fibrous additives such as cotton dust also contribute to surface stabilization, although their effect is generally lower compared with lignosulfonates (Butler et al., 2023; Sykorova et al., 2024).

Overall, binder incorporation significantly improves pellet handling characteristics and reduces material loss.

d) Hygroscopic Behavior

The hygroscopic behavior of pellets is strongly influenced by binder type. Some binders increase the pellet's tendency to absorb moisture, while others reduce hygroscopicity by creating more compact or hydrophobic structures.

Starch-based binders may increase moisture uptake due to their hydrophilic nature and strong affinity for water molecules. When added at higher proportions, starch can increase the equilibrium moisture content of pellets, negatively affecting storage stability and promoting swelling or surface softening.

In contrast, fiber-rich binders such as cotton dust, agricultural fines, or other cellulose-rich materials tend to reduce hygroscopicity by enhancing mechanical interlocking and creating denser microstructures with fewer open pores. These additives improve water resistance by minimizing capillary pathways within the pellet matrix (Ahn et al., 2014; Wang et al., 2020; Suvunnapob et al., 2015).

Overall, hygroscopic behavior depends on the hydrophilicity of the binder and its effect on pellet porosity and microstructure.

4.2 Thermal and Chemical Effects

a) Higher Heating Value (HHV)

Binders influence the calorific value of biomass pellets depending on their chemical composition and combustion characteristics.

Organic binders, such as starch, molasses, bio-oils, and crude glycerol, generally increase or maintain the higher heating value (HHV) because they contain combustible carbon-rich components. These binders enhance thermal stability and contribute additional energy during combustion.

In contrast, inorganic binders (e.g., bentonite, clay, cement dust, kaolin) increase the ash content and introduce non-combustible mineral matter. This results in lower HHV and reduced

energy density, making inorganic binders less desirable for high-quality fuel pellets where energy efficiency is critical (García-Maraver et al., 2011; Tumuluru, 2014; Bala-Litwiniak & Radomiak, 2019).

Therefore, selecting organic binders is generally preferred for applications where maintaining or improving HHV is essential.

b) Ash Content and Ash Behavior

Ash content and ash behavior are critical parameters in pellet quality classification because they directly affect slagging, fouling, and emission performance during combustion. The influence of binders on ash depends strongly on their origin and chemical composition.

Organic binders, such as starch, molasses, plant oils, bio-oils, and glycerol, typically contribute negligible additional ash due to their predominantly carbon–hydrogen–oxygen composition. Therefore, they do not significantly alter ash content and generally maintain compliance with premium pellet standards.

In contrast, inorganic binders (e.g., bentonite clay, kaolin, cement dust, dolomite) introduce substantial mineral matter into the pellet matrix. These materials can increase ash content by several percentage points, often exceeding the limits defined in ISO 17225-2, which classifies premium pellets (A1/A2) based on strict ash thresholds (typically <0.7–1.2% for A1 and <1.5% for A2). Elevated ash from inorganic additives may downgrade pellets to lower fuel classes.

Ash behavior (softening temperature, slagging tendency) is also negatively affected by inorganic binders due to increased silica, alumina, and metal oxides (García-Maraver et al., 2011; Gilbert et al., 2009).

c) Combustion and Emissions

Binders also influence combustion stability, volatile release patterns, and emission profiles. These effects depend on binder composition and chemical reactivity.

Molasses

Molasses contains high levels of sugars and volatile organic compounds. During combustion, these components promote rapid devolatilization, which can increase CO emissions, especially under suboptimal air–fuel ratios. Studies on briquettes containing molasses consistently report slightly elevated CO levels compared to unmodified biomass fuels.

Glycerol / Crude Glycerin

Glycerol improves combustion uniformity by acting as a thermal stabilizer. Its hydroxyl-rich molecular structure promotes controlled ignition and steady flame propagation. Glycerol-blended pellets exhibit reduced CO fluctuations and smoother temperature profiles during combustion.

Cotton Dust

Cotton dust consists mainly of cellulose and hemicellulose and contains very low ash (0.5–1.5%) without alkali-metal impurities that lower ash melting points. Therefore, cotton-dust-based blends do not negatively affect ash fusion temperature and show favorable ash behavior compared to agricultural residues with high silica (Suvunnapob et al., 2015; Bala-Litwiniak & Radomiak, 2019).

4.3 Effects on the Production Process

Binders influence multiple process-related parameters during pelletization, including energy consumption, die temperature, plugging behavior, and overall production efficiency. Their impact is closely tied to binder viscosity, lubricity, thermal characteristics, and interaction with biomass polymers.

a) Energy Consumption

Energy consumption during pelletization is largely determined by die friction**,** feedstock flowability**,** and plastic deformation capacity**.**

Oils and lipid-based binders

Vegetable oils and similar lipid-based additives act as natural lubricants, reducing die–particle friction. Lower friction translates directly to reduced specific energy consumption (SEC) per kilogram of pellets produced. Oils also smoothen particle sliding, reducing wear on the die surface.

Glycerol / Crude Glycerin

Glycerol behaves as a plasticizer, lowering the glass transition temperature of lignocellulosic polymers. This enhances flowability and reduces mechanical resistance inside the die channel. As a result:

- motor load decreases
- pelletizer torque is reduced
- SEC can drop by 10–25% depending on dosage

These effects contribute to more efficient compaction with less mechanical force (Tumuluru, 2014; Emami et al., 2015).

b) Die Temperature and Plugging

The pellet die is subject to thermal and mechanical loads, and its performance depends heavily on binder–biomass interactions.

Binders that reduce friction

Lubricating additives (oils, glycerol) reduce frictional heat generation, leading to lower die temperature. Reduced hot-spots help prevent thermal degradation of biomass polymers and improve pellet surface quality.

Binders that improve plasticity and cohesion

Starch, lignosulfonates, and bio-oil soften biomass fibers and improve compaction behavior, aiding uniform passage through die channels and minimizing plugging or choking events**.**

Inadequate or overdosed binders

Very sticky binders (e.g., excessive molasses) may increase die fouling and raise the risk of plugging if moisture conditions are not optimized.

Overall, proper binder selection stabilizes die temperature profiles and reduces downtime associated with clogging (Stelte et al., 2011; Gilbert et al., 2009).

c) Production Efficiency

Binder addition often improves overall production performance by enhancing feedstock processability and stabilizing pellet formation.

Higher throughput

Reduced friction and improved flowability result in smoother material transport through the conditioning and die sections. Many binders increase production throughput by:

- reducing torque
- increasing feed rate
- decreasing downtime

More stable pelletization

Organic binders provide improved cohesion and plasticity, yielding more uniform pellets with fewer defects. This translates into:

- fewer machine interruptions
- consistent die pressure
- optimized pellet length and density
- reduced fines accumulation in the system

When used correctly, binders offer an economic advantage by improving operational stability and lowering maintenance requirements (Kaliyan & Morey 2010; Bala-Litwiniak & Radomiak, 2019).

5. General Applications and Representative Studies on Binders

Numerous experimental and review studies have investigated the effects of different binder types on pellet quality across a wide range of biomass feedstocks. The collective findings of the literature demonstrate that binder type**,** application rate**,** and feedstock properties (e.g., lignin content, particle size, ash composition, moisture) are the dominant factors governing pellet mechanical durability, density, fines generation, ash characteristics, and combustion behavior.

Organic binders such as starch, molasses, crude glycerol, lignosulfonates, and bio-oils are widely used because they improve pellet cohesion, reduce friction during densification, enhance mechanical durability, and generally maintain or increase heating value. Studies by Nielsen et al. (2009), Ahn et al. (2014), and Bala-Litwiniak & Radomiak (2019) highlight that these binders can significantly increase durability (10–40%) and reduce fines by up to 50% at low dosages.

Fiber-rich agricultural additives, including wheat straw fines, corn stover, and cotton dust, have also been shown to promote mechanical interlocking and improve pellet structure (Gilbert et al., 2009; Suvunnapob et al., 2015). These materials typically have low ash content and minimal impact on combustion performance, making them suitable for co-pelletization with woody biomass.

In contrast, inorganic binders such as bentonite, kaolin, and cement dust are less desirable for fuel pellet production due to their tendency to increase ash content and decrease heating value. ISO 17225-2 quality standards place strict limits on ash levels, and even small additions of mineral binders can downgrade pellets from premium classes (A1/A2).

Recent studies have expanded the understanding of binder effects, especially in torrefied or mixed feedstocks. Works by Butler et al. (2023), and Sykorova et al. (2024) emphasize that binder–feedstock interactions depend strongly on thermal pretreatment, polymer softening behavior, and ash chemistry.

Overall, the literature demonstrates that no single binder is universally optimal. Instead, the effectiveness of a binder depends on its compatibility with the biomass matrix, its impact on pelletization energy demand, and its influence on the final fuel's physical and combustion properties.

5.1 Studies on Starch-Based Binders

Starch is one of the most widely studied and applied natural binders in biomass pelletization due to its low cost, availability, and strong adhesive properties. Its binding mechanism is primarily attributed to gelatinization, a process in which starch granules swell and form a viscous, cohesive matrix when exposed to heat and moisture during pelletization.

Ahn et al. (2014) conducted one of the most detailed investigations on starch-modified wood pellets. Their findings demonstrated that:

- Mechanical durability increased by approximately 10–25%, depending on binder dosage.
- Fines generation decreased significantly due to improved inter-particle bonding.

- Moisture uptake increased, as starch is highly hydrophilic and absorbs water readily.

Similarly, Kaliyan and Morey (2010) highlighted starch's ability to form strong solid bridges during densification. They reported that starch-based binders improve pellet integrity by promoting plastic deformation and enhancing adhesion between lignocellulosic particles.

In addition, Mani et al. (2006) confirmed the effectiveness of starch during densification, attributing its strong adhesive role to gelatinization under elevated temperatures. Their work emphasized that starch improves compaction behavior and contributes to reduced die friction at optimal moisture levels. Mani et al. also noted that starch reduces die friction when moisture is within the optimal range (10–15%).

Overall, the literature consistently supports the use of starch as an effective natural binder that improves mechanical performance, although its hydrophilic nature can negatively influence hygroscopic stability during storage.

5.2 Lignosulfonate in Pelletization

Lignosulfonates, derived from the sulfite pulping process, are among the most effective and widely used industrial binders for biomass pelletization. Their superior performance is attributed to their thermoplastic behavior**,** high molecular weight**,** and ability to form solid bridges between lignocellulosic particles during compression.

Extensive experimental work by Nielsen et al. (2009) and Stelte et al. (2011) has clearly demonstrated the advantages of lignosulfonate addition in pellet production:

- Mechanical durability increases by 20–40%**,** even at low inclusion rates.
- Fines generation can be reduced by up to 50%, due to strong cohesive bonding and smoother pellet surfaces.
- Die lubrication is improved, as lignosulfonates lower friction between the die wall and biomass particles, reducing energy consumption and thermal stress.
- Very low dosage levels (0.5–2 wt%) are sufficient for significant improvements, making lignosulfonates highly economical for industrial application.

Because lignosulfonates enhance process stability, reduce wear on pellet mill components, and improve operational throughput, they are especially advantageous in commercial-scale pellet mills**,** where feedstocks may vary in quality and large volumes require consistent densification performance.

Overall, lignosulfonates remain one of the most effective binder options for high-quality pellet production, particularly when durability, fines control, and process efficiency are prioritized.They are particularly effective when densifying low-lignin feedstocks such as agricultural residues, where natural binding mechanisms are insufficient.

5.3 Glycerol and Crude Glycerin

Glycerol and crude glycerin, major by-products of biodiesel production, have gained significant interest as low-cost and effective pellet binders. Their molecular structure—rich in hydroxyl groups—enables plasticization**,** improved flowability, and enhanced bonding within lignocellulosic matrices.

Experimental studies show that glycerol modifies pelletization behavior through the following mechanisms:

- ✓ *Reduced die friction*

Glycerol acts as a lubricant and plasticizer, lowering friction between biomass particles and the die wall.
This results in smoother pellet formation and reduced mechanical resistance.

- ✓ *Lower energy consumption (≈10–25%)*

Emami et al. (2015) and Marrugo et al. (2019) demonstrated that crude glycerol reduces specific energy consumption (SEC) during densification due to improved particle deformability.

- ✓ *Improved pellet density*

Bala-Litwiniak & Radomiak (2019) showed that adding 2–7% waste glycerol yields more compact, denser pellets with enhanced structural uniformity**.**

- ✓ *Excessive amounts may soften pellets*

At higher dosages (>7–10%), glycerol's strong plasticizing effect can lead to over-softening, reducing mechanical durability and increasing deformation during storage.

Overall, glycerol is considered one of the most efficient industrial binder candidates, especially in mixed biomass systems and large-scale mills seeking to reduce pelletization energy costs (Emami et al., 2015; Marrugo et al., 2019; Bala-Litwiniak & Radomiak, 2019).

5.4 Molasses and Sugar-Rich Binders

Molasses is a sugar-rich by-product of the sugar industry and has been extensively evaluated as a cost-effective binder for biomass densification. Its high content of sucrose, glucose, fructose, and various organic compounds gives it excellent adhesive potential during pelletization. When heated, these sugars undergo caramelization and thermal polymerization, forming strong solid bridges between particles.

Numerous studies have shown that molasses can significantly improve pellet quality. Its viscous nature enhances particle cohesion, while the sugars act as natural adhesives during compaction and cooling.

Key findings from experimental research include:

- ✓ *Increased durability*

Molasses consistently improves mechanical durability due to enhanced particle bonding and reduced surface cracking. Many briquette and pellet studies report substantial gains in durability at relatively low inclusion rates (3–8%).

- ✓ *Reduced fines*

Because of its strong binding action and surface coating ability, molasses effectively reduces fines generation during handling and transport. Pellets exhibit smoother surfaces and improved abrasion resistance.

- ✓ *Potential increase in CO emissions*

The high sugar content leads to rapid devolatilization during combustion. Under suboptimal air–fuel conditions, this can increase CO emissions, a finding supported by combustion studies on molasses-bound briquettes. Therefore, while molasses improves physical quality, its combustion profile must be carefully evaluated**.**

- ✓ *Effective but requires combustion behavior analysis*

Given its strong adhesive characteristics, molasses is an effective binder for improving durability and reducing material losses, but its influence on emissions and ash chemistry must be assessed to ensure compliance with fuel standards (García-Maraver et al., 2011).

5.5 Fiber-Based and Agricultural Residue Binders

Fiber-rich agricultural residues—including straw fines, rice husk powder, corncob particles, and other lignocellulosic by-products—have received increasing attention as cost-effective natural binders in biomass pelletization. Their high cellulose and hemicellulose content promotes mechanical interlocking, enhancing particle–particle cohesion during densification.

Research on agricultural fines consistently demonstrates several advantages:

Stelte et al. (2011) and Gilbert et al. (2009) showed that fiber-rich residues contribute to the formation of a reinforcing structural network within the pellet matrix. This improves pellet integrity, enhances mechanical durability, and reduces breakage during handling. Unlike inorganic binders, agricultural fines introduce little to no additional ash, keeping fuel quality within acceptable limits.
Ajimotokan et al. (2019) demonstrated that composite briquettes made from rice husk and corncob maintain ash contents compatible with standard biomass fuel classes, while also showing improved strength and compaction behavior.

Table 5.1. Summary of Key Findings From Representative Binder Studies

Binder Type	Positive Effects	Negative Effects / Limitations	Key References
Starch	• Durability ↑ (10–25%) • Strong gelatinization → solid bridging • Fines ↓ • Improved compaction	• Highly hydrophilic → moisture uptake ↑ • Storage stability ↓	Ahn et al., 2014; Kaliyan & Morey, 2010; Mani et al., 2006
Lignosulfonates	• Durability ↑ (20–40%) • Fines ↓ up to 50% • Die lubrication ↑ • Works at low dosage (0.5–2%)	• Slight ash increase • Color darkening possible	Nielsen et al., 2009; Stelte et al., 2011
Glycerol / Crude Glycerin	• SEC ↓ (10–25%) • Density ↑ • Flowability ↑ • Improved heat transfer during compaction	• Over-dosage → pellet softening • CO emissions slight ↑	Emami et al., 2015; Marrugo et al., 2019; Bala-Litwiniak & Radomiak, 2019
Molasses	• Durability ↑ • Fines ↓ • Strong surface adhesion • Effective at 3–8%	• CO emissions ↑ • Sticky behavior → handling issues	García-Maraver et al., 2011
Bio-oils / Pyrolytic Lignin	• Thermoplastic softening • Density ↑ • Mechanical bonding ↑	• Moisture variability • Odor & color darkening	Hu et al., 2015
Fiber-Based Residues (cotton dust, straw fines, corncob, rice husk)	• Interlocking ↑ • Durability ↑ • Ash stable (low increase) • Very low cost, highly available	• Low thermoplasticity • Rice husk silica ↑ (if high ratios used)	Gilbert et al., 2009; Suvunnapob et al., 2015; Ajimotokan et al., 2019; Sarker et al., 2023
Inorganic Binders (bentonite, kaolin, cement dust)	• Shape stability ↑ • Bridging ↑ (mineral bonding)	• Ash ↑↑ • HHV ↓ • Not suitable for premium pellets (ISO 17225-2 limits)	García-Maraver et al., 2011; Gilbert et al., 2009

Agricultural residues are abundant, inexpensive, and readily available in major crop-producing regions.

Sarker et al. (2023) highlighted their suitability as economical binder alternatives for large-scale pellet and briquette manufacturing, especially when blended with woody biomass to compensate for lower lignin levels.

Fiber-based binders offer a practical and economically attractive strategy for improving pellet quality. They enhance inter-particle bonding, maintain acceptable ash levels, and provide cost-effective solutions for industrial-scale operations, particularly in regions with large agricultural processing industries.

6. Conclusion

Binders play an essential role in defining the physical, mechanical, chemical, and combustion-related properties of biomass pellets. Extensive literature demonstrates that the strategic use of binders greatly enhances pellet quality, particularly when dealing with low-lignin, high-ash, or structurally weak feedstocks. Natural binders (e.g., starch, lignosulfonates), industrial and organic binders (e.g., glycerol, bio-oils), and agricultural residue–based binders (fiber-rich powders) improve pellet durability, density, and surface integrity through a variety of bonding mechanisms, including gelatinization, chemical bridging, plasticization, and mechanical interlocking.

Effective binder selection must consider feedstock composition**,** target pellet class**,** processing conditions, and economic practicality. Most studies indicate that optimal binder dosages fall within the 0.5–5% range; higher concentrations may lead to undesirable effects such as increased hygroscopicity, softening, or elevated ash content. When appropriately applied, binders reduce specific energy consumption during pelletization, enhance die lubrication, and decrease fines and abrasion during handling and transport.

Overall, binders offer multiple performance advantages:

- Increased mechanical durability
- Improved density and compaction behavior
- Reduced fines and abrasion
- Enhanced process stability and efficiency
- More uniform and controlled combustion characteristics

Consequently, a deep understanding of binder mechanisms, pellet–binder interactions, and process optimization is critical for the continued advancement of biomass densification technologies. Future research should focus on the thermochemical behavior**,** microstructural bonding phenomena**,** and long-term performance of low-cost and waste-derived binders, with particular emphasis on developing sustainable, high-efficiency formulations suitable for industrial-scale pellet production. Particular emphasis should be placed on binder performance under varying moisture regimes and high-throughput industrial pelletization settings.

KAYNAKLAR

Adapa, P., Tabil, L., & Schoenau, G. (2009). Compaction characteristics of barley, canola, oat and wheat straw. *Biosystems engineering*, *104*(3), 335-344.

Ahn, B. J., Chang, H. S., Lee, S. M., Choi, D. H., Cho, S. T., Han, G. S., & Yang, I. (2014). Effect of binders on the durability of wood pellets fabricated from Larix kaemferi C. and Liriodendron tulipifera L. sawdust. *Renewable energy*, *62*, 18-23.

Ajimotokan, H. A., Ibitoye, S. E., Odusote, J. K., Adesoye, O. A., & Omoniyi, P. O. (2019). Physico-mechanical properties of composite briquettes from corncob and rice husk. *Journal of Bioresources and Bioproducts*, *4*(3), 159-165.

Anukam, A., Berghel, J., Henrikson, G., Frodeson, S., & Ståhl, M. (2021). A review of the mechanism of bonding in densified biomass pellets. *Renewable and Sustainable Energy Reviews*, *148*, 111249.

Bala-Litwiniak, A., & Radomiak, H. (2019). Possibility of the utilization of waste glycerol as an addition to wood pellets. *Waste and Biomass Valorization*, *10*(8), 2193-2199.

Butler, J. W., Skrivan, W., & Lotfi, S. (2023). Identification of optimal binders for torrefied biomass pellets. *Energies*, *16*(8), 3390.

Christoforou, E., & Fokaides, P. A. (2016). A review of olive mill solid wastes to energy utilization techniques. *Waste Management*, *49*, 346-363.

Emami, S., Tabil, L. G., & Adapa, P. (2015). Effect of glycerol on densification of agricultural biomass. *International Journal of Agricultural and Biological Engineering*, *8*(1), 64-73.

Espinoza-Tellez, T., Montes, J. B., Quevedo-León, R., Valencia-Aguilar, E., Vargas, H. A., Díaz-Guineo, D., ... & Díaz-Carrasco, O. (2020). Agricultural, forestry, textile and food waste used in the manufacture of biomass briquettes: a review. *Scientia Agropecuaria*, *11*(3), 427-437.

García-Maraver, A., Popov, V., & Zamorano, M. (2011). A review of European standards for pellet quality. *Renewable Energy*, *36*(12), 3537-3540.

García Martín, J. F., Cuevas, M., Feng, C. H., Álvarez Mateos, P., Torres Garcia, M., & Sánchez, S. (2020). Energetic valorisation of olive biomass: Olive-tree pruning, olive stones and pomaces. *Processes*, *8*(5), 511.

Gilbert, P., Ryu, C., Sharifi, V., & Swithenbank, J. (2009). Effect of process parameters on pelletisation of herbaceous crops. *Fuel*, *88*(8), 1491-1497.

Goh, C. S., Junginger, M., Cocchi, M., Marchal, D., Thrän, D., Hennig, C., ... & Deutmeyer, M. (2013). Wood pellet market and trade: a global perspective. *Biofuels, Bioproducts and Biorefining*, *7*(1), 24-42.

Hu, Q., Shao, J., Yang, H., Yao, D., Wang, X., & Chen, H. (2015). Effects of binders on the properties of bio-char pellets. *Applied Energy*, *157*, 508-516.

Jordan, M., Lenz, V., Millinger, M., Oehmichen, K., & Thrän, D. (2019). Future competitive bioenergy technologies in the German heat sector: Findings from an economic optimization approach. *Energy*, *189*, 116194.

Kaliyan, N., & Morey, R. V. (2010). Natural binders and solid bridge type binding mechanisms in briquettes and pellets made from corn stover and switchgrass. Bioresource technology, 101(3), 1082-1090.

Lizundia, E., Sipponen, M. H., Greca, L. G., Balakshin, M., Tardy, B. L., Rojas, O. J., & Puglia, D. (2021). Multifunctional lignin-based nanocomposites and nanohybrids. *Green Chemistry*, *23*(18), 6698-6760.

Mani, S., Tabil, L. G., & Sokhansanj, S. (2006). Effects of compressive force, particle size and moisture content on mechanical properties of biomass pellets from grasses. *Biomass and bioenergy*, *30*(7), 648-654.

Marrugo, G., Valdés, C. F., Gómez, C., & Chejne, F. (2019). Pelletizing of Colombian agro-industrial biomasses with crude glycerol. *Renewable Energy*, *134*, 558-568.

Matúš, M., Križan, P., Šooš, Ľ., & Beniak, J. (2018). The effect of papermaking sludge as an additive to biomass pellets on the final quality of the fuel. *Fuel*, *219*, 196-204.

Nielsen, N. P. K., Holm, J. K., & Felby, C. (2009). Effect of fiber orientation on compression and frictional properties of sawdust particles in fuel pellet production. *Energy & Fuels*, *23*(6), 3211-3216.

Oladeji, J. T. (2010). Fuel characterization of briquettes produced from corncob and rice husk resides. *The Pacific Journal of Science and Technology*, *11*(1), 101-106.

Sam Obu, C. V., Amos, J., Chris-Ukaegbu, S. O., Dike Chijindu, P., & Odeniyi, O. M. (2022). Production of Fuel Briquettes from a Blend of Corn cob and Rice husk. *International Journal of Research and Review*, *9*(2), 349-978.

Samuelsson, R., Larsson, S. H., Thyrel, M., & Lestander, T. A. (2012). Moisture content and storage time influence the binding mechanisms in biofuel wood pellets. *Applied energy*, *99*, 109-115.

Sarker, T. R., Borugadda, V. B., Meda, V., & Dalai, A. K. (2023). Optimization of pelletization process conditions and binder concentration for production of fuel pellets from oat hull and quality evaluation. *Biomass and Bioenergy*, *174*, 106825.

Serrano, C., Monedero, E., Lapuerta, M., & Portero, H. (2011). Effect of moisture content, particle size and pine addition on quality parameters of barley straw pellets. *Fuel processing technology*, *92*(3), 699-706.

Ståhl, M., Berghel, J., Frodeson, S., Granström, K., & Renström, R. (2012). Effects on pellet properties and energy use when starch is added in the wood-fuel pelletizing process. *Energy & Fuels*, *26*(3), 1937-1945.

Stelte, W., Clemons, C., Holm, J. K., Sanadi, A. R., Ahrenfeldt, J., Shang, L., & Henriksen, U. B. (2011). Pelletizing properties of torrefied spruce. *biomass and bioenergy*, *35*(11), 4690-4698.

Strezov, V., & Anawar, H. M. (2019). *Renewable Energy Systems from Biomass*. Boca Raton FL: CRC Press.

Suvunnapob, S., Ayudhya, B. I. N., & Kusuktham, B. (2015). A study of cotton dust mixed with wood dust for bio-briquette fuel. *Engineering Journal*, *19*(4), 57-70.

Sykorova, V., Jezerska, L., Sassmanova, V., Honus, S., Peikertova, P., Kielar, J., & Zidek, M. (2024). Biomass pellets with organic binders-before and after torrefaction. *Renewable Energy*, *221*, 119771.

Tumuluru, J. S. (2014). Effect of process variables on the density and durability of the pellets made from high moisture corn stover. *Biosystems engineering*, *119*, 44-57.

Ungureanu, N., Vladut, V., Voicu, G., Dinca, M. N., & Zabava, B. S. (2018). Influence of biomass moisture content on pellet properties–review. *Eng. Rural Dev*, *17*, 1876-1883.

Wang, Z., Zhai, Y., Wang, T., Wang, B., Peng, C., & Li, C. (2020). Pelletizing of hydrochar biofuels with organic binders. *Fuel*, *280*, 118659.

CHAPTER 2

THERMAL BUCKLING ANALYSIS OF THIN COMPOSITE LAMINATES

Sait Özmen ERUSLU[1]

1 Doç.Dr., Tekirdağ Namık Kemal Üniversitesi, Çorlu Mühendislik Fakültesi, Makine Mühendisliği Bölümü,ORCID: 0000-0003-2942-378X, oeruslu@nku.edu.tr

1. INTRODUCTION

Fiber-reinforced composite materials are widely used as structural elements in engineering applications due to their exceptional strength-to-weight ratio, along with good damping characteristics and excellent fatigue resistance. Since materials in such applications are often exposed to high temperatures and stresses, they must perform efficiently and maintain their stability under environmental conditions. For this reason, composite materials are preferred where high performance and stability are required under extreme conditions.

Textile composites are generally defined as structures formed by combining polymer-based matrix materials with textile-based reinforcement elements. Compared to conventional fiber-reinforced products, the main advantages of textile composites are their ability to provide balanced reinforcement within the structure and the ease and low cost of obtaining reinforcement materials [1].

The textile reinforcements consist of interlaced structures made from yarns and products derived from yarns. With the development of modern textile processing technologies, it has become possible to produce high-quality and multifunctional reinforcement elements.

In particular, in the aerospace industry, the high level of discontinuities in conventional laminated composites increases interlaminar stresses [2]. Since textile composites do not exhibit such discontinuities, delamination between layers is not observed, especially in braided textile composites.

Textile composites find extensive applications across the aerospace, marine, defense, automotive, construction, and energy sectors. The reinforcement elements in textile composites can be produced in various forms such as braided, woven, or nonwoven structures. Common reinforcement fibers include glass fiber, carbon fiber, polyester fiber, and aramid fiber. As for matrix materials, polymer-based resins, polyurethane foam, and thermoplastic materials (such as polypropylene and polyethylene) are typically used.

The behavior of textile-based materials under thermal loads varies depending on their micromechanical structure, which is influenced by the geometric characteristics of the material. Therefore, there has been a growing need to investigate the micromechanical structure of textile composites. Micromechanics-based approaches in textile composites date back to the 1980s, when when Yoshino and Ohtsuka conducted a two-dimensional finite element study employing plane strain elements and a unit-cell method to simulate intricate yarn architectures.[3].

In the mid-1980s, with the development of micromechanical models, stress fields under thermo-mechanical loads in continuous fiber-reinforced composites were identified. By the late 1980s, parallel to the advancements in textile manufacturing technologies, the first micromechanical models for woven composites were developed by Chou and his colleagues [4]. During this period, the coefficients of thermal expansion and thermal bending in two-dimensional woven composites were also determined through micromechanical models.

Non-crimp fabric (NCF) reinforced composites are composed of reinforcement elements created by stacking yarns in the thickness direction and stitching them together. NCF-reinforced composites exhibit higher compressive strength compared to woven textile composites [5]. Drapier S. et al. investigated the interlaminar shear strength and compressive strength of NCF composites using the finite element method and found that their compressive strength was higher than that of other woven composites [6].

With the advancement and widespread adoption of carbon and aramid material manufacturing techniques, their use in textile composites has become more common.NCF composites made from carbon fiber and kevlar yarn offer high temperature resistance, high compressive strength, and structural stability. Composites reinforced with Carbon-Carbon, Aramid-Aramid, or Carbon-Aramid fibers find extensive applications due to their high-temperature resistance (up to 1500°C) and low specific weight.

The earliest studies on thermal deformation in composite materials were based on energy principles. In the 1970s, the coefficients of thermal expansion for fiber-reinforced composites were determined. Scharpery determined the coefficient of thermal expansion for both isotropic and anisotropic composites containing isotropic phases [7]. In two-phase woven composites, the coefficients of thermal expansion in the longitudinal and transverse directions were defined by Ishikawa and coworkers using one- and two-dimensional micromechanical models [8]. Rogers et al. defined the longitudinal and transverse coefficients of thermal expansion for transversely arranged fiber reinforcements within an isotropic matrix based on the Chamberlain equations [9],[10]. In the 1980s, the determination of thermal expansion coefficients in fiber-reinforced materials accelerated research on thermal deformation. Reddy and colleagues investigated the deformations and stresses in the thickness direction of laminated composite plates [11-13].

Research on thermal buckling of composite plates increased during the 1990s. These studies generally employed large-deformation theories and examined the effects of transverse shear deformations on critical buckling parameters and buckling mode shapes. From the 2000s onward, thermal buckling studies have focused primarily on different types of composite materials. Some studies investigated the temperature-dependent variation of material properties in composite and sandwich plates and analyzed the effects of viscoelastic and hygroscopic behavior on thermal buckling results. Babu C. S. et al. studied the thermal buckling behavior of materials made from composite and sandwich plates using large-deformation theories. [14]. Jones R. M. et al. demonstrated that, considering the effects of hygroscopic and thermal influences on critical thermal buckling temperatures, some laminates buckle during cooling rather than heating, depending on boundary conditions [15]. Similarly, Aydogdu determined the critical thermal buckling temperatures of laminated composite beams based on the ratio of thermal expansion coefficients in orthotropic directions, showing that some beams buckle during cooling while others buckle during heating [16]. Pradeep V. et al. investigated the vibration and thermal buckling parameters of multilayered viscoelastic sandwich plates [17]. Matsunaga H. et al. conducted a study on the thermal buckling analysis of structures composed of angled-layered laminated composites and sandwich plates [18]. Research on thin-walled laminated shell-based beams and laminated composites in smart structures under electric and magnetic fields remains active, particularly regarding their buckling and vibration behavior [19–20]. Thermal buckling of hybrid metal/composite panels has also received significant attention, with Ahmed et al. [21] showing that machine learning can predict the behavior of

laminated composite plates under mechanical and thermal loads, while Deng et al. [22] verified analytical, numerical, and experimental methods for accurately predicting the thermal buckling of hybrid metal/composite panels under aircraft temperature conditions. Numerical and analytical solutions for thermal buckling using classical and higher-order laminated plate theories are still being investigated. Eruslu et al. studied short fiber-reinforced laminated composite plates, considering the orthotropy and aspect ratios of both plates and fibers for cross-ply laminates [23]. Baran et al. examined how ply orientation influences the thermal buckling behavior of laminated plates using both analytical and numerical approaches [24]. Emrullah analyzed the thermal buckling of laminated plates with varying fiber volume fractions through the differential quadrature method and finite element modeling [25]. Finite element analysis (FEA) is a commonly employed approximate technique that yields results in close agreement with analytical solutions for thin plates and shell-based structures under various boundary conditions [26].

Although laminated composites are generally used as multilayer structural elements in practical applications, they are also widely employed as thin layers in sandwich composites and, in particular, as coating materials in woven or non-crimp textile composites. Accordingly, in this chapter, both experimental and numerical analyses of the thermal buckling behavior of thin laminated composites were conducted.

2. Experimental Study

The composite materials were manufactured using the vacuum infusion method, which was carried out in the laboratory using the setup shown below [1].

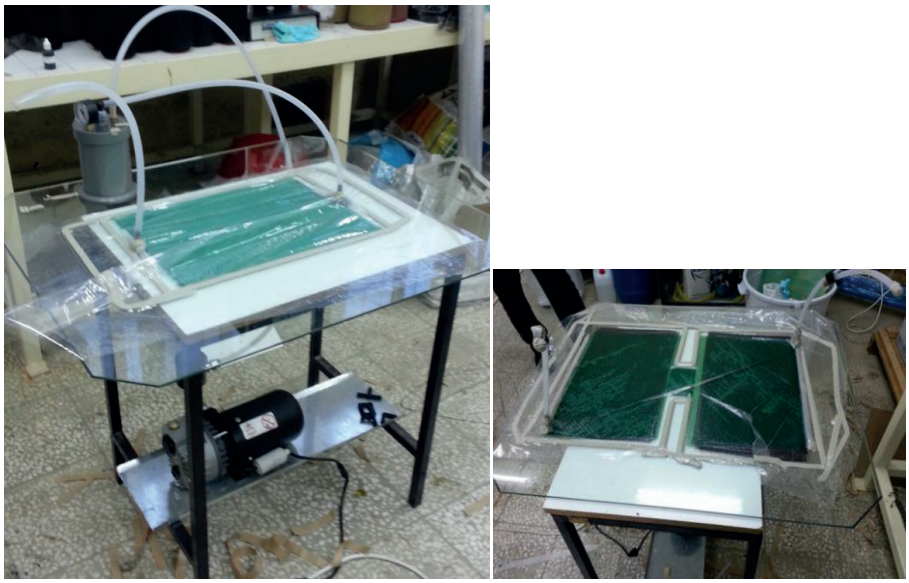

Figure 1. Vacuum infusion setup used at composites production

In this study, an infusion-type vinylester resin, designated as Polives 702, was used as the matrix phase,the mechanical properties of vinlester resin is given in Table 1. In the first stage, composite plates of Woven Carbon, Woven Aramid-Carbon Epoxy, and NCF Carbon Epoxy were fabricated using the vacuum infusion method and subsequently subjected to a curing process. The mechanical properties of the fabrics obtained from the manufacturer and used in the study are presented in Table 2 [1]. Tensile specimens were then prepared from the produced composites along orthotropic directions (0°, 90°, and 45°) for mechanical characterization. In

textile composites, these testing directions are referred to as the Machine Direction, Warp Direction, and Weft Direction. To ensure that the lamina specimens met the minimum thickness requirement for tensile testing according to ASTM D3039, four-layered specimens with a thickness greater than 1 mm were selected for mechanical characterization. The mechanical properties of the produced specimens obtained from the tensile tests are presented in Table 3.

Table 1: Mechanical properties of vinlester resin

Material	Elastic Modulus (MPa)	Tensile Strength (MPa)	Elongation at Break %	Density [g/cm3]	Termal Expansion Coefficient [10^{-6}/K]
Vinlester Resin	3000	76	5	1	10

Table 2: Mechanical properties of textile fabrics employed in composite production.

Fiber Properties	Plain Weave Carbon Fabric 	Plain Weave Aramid Fabric 	Non Crimp Carbon Fabric 
Fiber diameter [µm]	7	5	5
Density [g/cm3]	1.76	1.10	3.00
Tensile Strength[MPa]	3950	3600	4000
Elastic modulus[GPa]	238.2	124	235
Termal Expansion Coefficient [10^{-6}/K]	-0,1	-2.1	-0.1
Elongation at Break (%)	1.9	2.4	1.8
Ply Orientation	0/90	0/90	+45/-45
Volume Fraction (%)	35	32	41.5
Ply Thickness (mm)	0.35	0.34	0.3

Table 3: Tensile test results of textile fabric epoxy composites

Textile Fabrics	Layer Number	Test Directions	Elastic Modulus (GPa)	Tensile Strength (MPa)	Elongation at Break %
Carbon Fabric	4	0°	22.319	460.181	4.067
		45°	7.353	105.755	33.247
		90°	22.308	460.1	4.06
Aramid - Carbon Fabric	4	0°	20.624	456.333	4.603
		45°	6.514	54.136	16.465
		90°	20.585	455.29	4.628
NCF Fabric	2	0°	6.518	28.118	4.857
		45°	23.053	185.847	5.534
		90°	5.745	24.500	4.23

In the second stage, specimens were prepared to investigate the thermal behavior of the produced plates, and heating and rapid cooling procedures were carried out in the thermal chamber shown below [1].

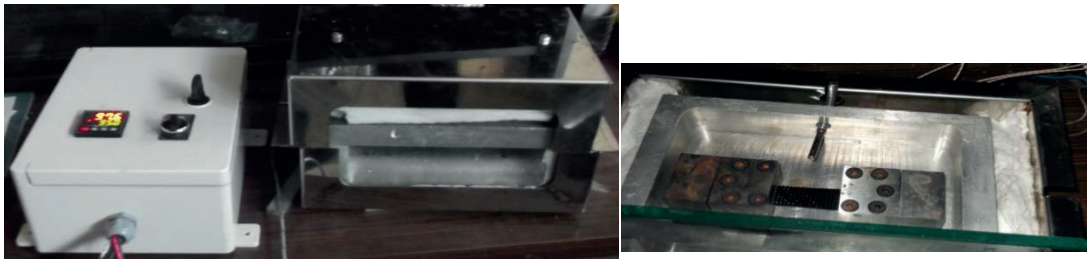

Figure 2. Thermal chamber and clamps used in the thermal buckling tests.

The specimens were fixed in the chamber using two small clamps designed to provide clamped boundary conditions at both ends. . The ambient temperature was recorded with a J-type precision thermocouple and relayed to the temperature control unit. The specimens were heated to a target temperature, maintained until thermal equilibrium was achieved, and subsequently rapidly cooled to 22 °C.

3. Determination of the Thermal Expansion Coefficients of Laminated Composites

When determining the temperature range, the thermal expansion coefficient of the specimens was calculated using rule of mixture equations based on the fiber and matrix phase thermal material properties. The thermal expansion coefficients of consitiuents of composites α_1 and α_2 have been theoretically defined in the literature.

Scharpery determined the thermal expansion coefficients for isotropic and anisotropic composites with isotropic phases [27]. For a two-phase composite, the longitudinal and transverse thermal expansion coefficients can be defined as follows [28].

$$\alpha_1 = \frac{E_f \alpha_f v_f + E_m \alpha_m v_m}{E_f v_f + E_m v_m} \quad (1)$$

$$\alpha_2 = (1+\vartheta_f)\alpha_f v_f + (1+\vartheta_m)\alpha_m v_m - \alpha_1(\vartheta_f v_f + \vartheta_m v_m) \quad (2)$$

In plain weave woven composites, using the rule of mixtures were obtained using the rule of mixtures given by the following equation.

$$\alpha_1 = \propto_2 = \propto_c = \frac{E_f \alpha_f v_f + E_m \alpha_m v_m}{E_f v_f + E_m v_m} \quad (3)$$

The calculated thermal expansion properties of laminated composites at the experiments are given as follow

Table 4: Thermal expansion coefficients of produced textile fabric epoxy laminated composites

Textile Fabric Epoxy Composites	Layer Number	Volume Fraction %	Thermal Expansion Coefficient $(10^{-6}/K)$
Carbon Fabric	4	35	1.918
Aramid-Carbon Fabric	4	32	1.761
NCF Fabric	2	41.5	1.51

The numerical analysis of the specimens was performed using the finite element method, and the thermal buckling temperatures were determined. The experimentally obtained results were compared with the numerical results to identify the thermal buckling temperature range. The plate dimensions used in the experimental studies were also adopted in the numerical calculations for finite element modeling, with the plate length and width specified as $a = 130$mm and $b = 30$mm, respectively.

4. Finite Element Modeling

A finite element model was developed in ANSYS using the laminated plate dimensions from the experiments, with boundary conditions replicating the clamping setup. The specimen was restrained along two edges, and a uniform temperature was applied up to the resin's melting point (120 °C), consistent with the analysis conditions (Figure 3).

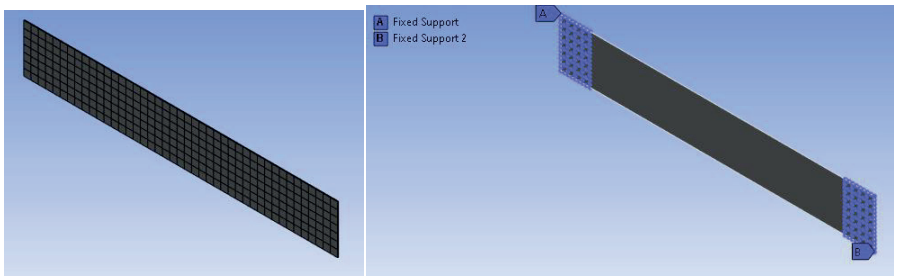

Figure 3. Finite element model a) Mesh b) Boundary conditions

The coupled-field analysis approach was employed, in which a static analysis was first performed to determine the prestress effects at the supports under a uniform temperature field. Subsequently, a buckling analysis was conducted to identify the critical buckling temperatures and corresponding mode shapes. Based on the convergence study, the mesh density was set to 200 elements. The convergence results are presented in Table 5 . The analysis was performed for [0°/90°] carbon fabric plain weave laminated composites produced experimentally. The plate dimensions were specified as $a = 130$ mm and $b = 30$ mm, respectively.

Table 5: Convergence Results at Finite Element Model

Element Size (mm)	Element Number	The Equivalent Von Mises Stress (MPa)	Critical Buckling Temperature T_{cr} (C°)
6	66	1.117	40.7
4	165	1.264	40.7
3	301	1.372	40.7
2	650	1.526	40.7

The convergence study indicated that the critical buckling temperature remained unchanged with an increasing number of elements, whereas the Von Mises stress increased due to stress singularities occurring at the fixed support boundaries, as shown in the figure below. An element size of 3 mm was selected, considering the variation in the Von Mises stress distribution.

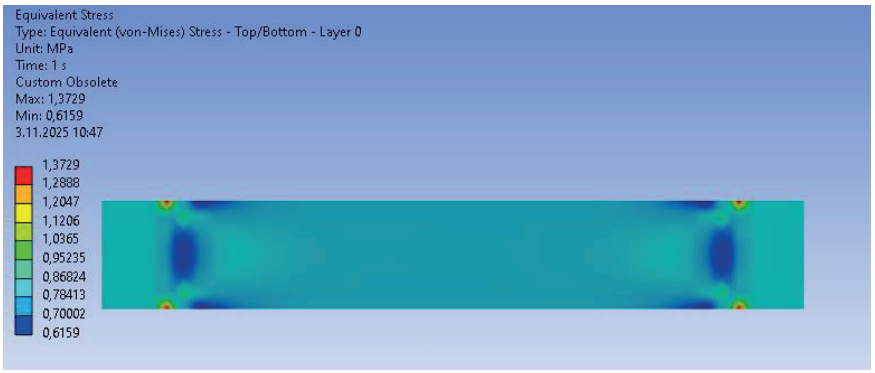

Figure 4. Stress singularity problem at the boundaries

In the analysis, the shell element SHELL181, which is an eight-node element with quadratic interpolation and six degrees of freedom per node, was used to account for the out-of-plane deformations resulting from prestress effects.

5. RESULTS AND DISCUSSION

In this study, the thermal buckling results from finite element analysis are compared with experimental findings. The influence of layer count, fabric type, and hybrid configurations on the thermal buckling behavior of laminated plates is examined. The critical buckling temperatures and their associated mode shapes are determined and reported.

5.1 Finite Element Analysis and Experimental Results

The finite element results for the critical thermal buckling temperatures of textile fabric laminated composites, considering the effect of the number of layers, are presented in Table 6. These results are compared with the experimental findings in the same table [29]. Temperatures above 120 °C were not considered, as this value corresponds to the glass transition temperature of the vinylester epoxy resin.

The results indicate that thermal buckling is significant for thinner woven fabric composites with thicknesses up to 0.5 mm. Two distinct buckling modes were observed for these thinner laminates. For composites with an increasing number of plies, the thermal buckling temperature exceeds the melting point of the vinylester epoxy. Some second-mode buckling responses were not captured experimentally due to temperature measurement limitations in the setup.

It was observed that the thermal expansion coefficients calculated using the Schapery-based rule of mixtures provided satisfactory results for isotropic-type composites, while a good correlation was obtained between the analytical and experimental results for the critical thermal buckling temperatures [28]. In hybrid carbon–aramid laminate combinations, the thermal buckling temperature decreased with an increasing number of aramid fabric plies, owing to their lower thermal expansion coefficients. The thermal buckling modes of the textile fabric laminates for thinner specimens are presented in the following figures for both the experimental and numerical results.

Table 6. Thermal buckling temperature results for textile fabric laminated composites

Textile Fabric Epoxy Composites	Layer Number	Thickness (mm)	Experimental Critical Buckling Temp. T_{cr} (C°) Mode1 Mode2	Numerical Critical Buckling Temp. T_{cr} (C°) Mode1 Mode 2	Numerical Critical Buckling Force (N)
Carbon Fabric	1	0.35	40.3 82.7	40.7 60	5.55 11.29
Carbon Fabric	2	0.52	72.6 -	63 106	18.10 37.09
Carbon Fabric	4	1.06	-	192	153.05
Aramid-Carbon Fabric	2	0.51	68.4 -	65 110	15.88 32.51
Aramid-Carbon Fabric	4	1.03	-	197	130.33
NCF Fabric	2	1.05	-	270	120.27

Figure 5. Thermal buckling modes for one layer carbon fabric laminates at experiments [1]

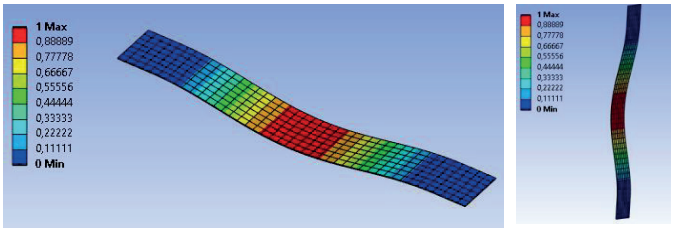

Figure6. Thermal buckling mode I one layer carbon fabric laminates at numerical analysis

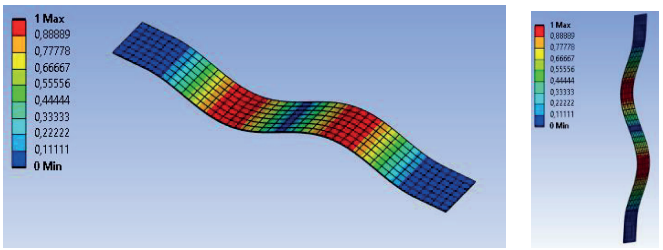

Figure 7. Thermal buckling mode II one layer carbon fabric laminates at numerical analysis

Figure 8. Thermally buckled two layer carbon-aramid fabric laminates [1]

When we present a comparison between the experimental results and numerical simulations, we observe close agreement in both the mode shapes and buckling patterns.The thermal buckling temperatures can be obtained more accurately in the experimental data by increasing the measurement precision.

6. CONCLUSIONS

Based on the experimental and finite element investigations of the thermal buckling behavior of textile fabric laminated composites, the following conclusions can be drawn.

Thermal buckling was found to be significant for thinner woven fabric laminates, particularly those with thicknesses below 0.5 mm, where multiple buckling modes can occur. In this study, only the first and second buckling modes were considered due to the melting limitations of vinylester epoxy. However, other buckling modes and relatively thicker laminates may be investigated in future studies, given advancements in epoxy resin technology that now allow materials to withstand temperatures up to 600 °C.

In hybrid carbon–aramid laminates, the thermal buckling temperature decreased with an increasing number of aramid plies due to their lower thermal expansion coefficients, demonstrating the influence of material combination on thermal stability.

NCF laminated composites have a higher fiber content and more uniform load transfer because the fibers are laid in biaxial directions without being interlaced. This arrangement allows for a higher fiber volume fraction and reduces the presence of voids. As a result, laminates produced using the vacuum infusion technique tend to be thicker compared to woven fabric laminates. Therefore, NCF laminated composites produced using this technique generally exhibit higher thermal buckling resistance compared to woven fabric laminates, making it important to consider alternative manufacturing methods—such as prepreg lay-up, compression molding, or resin transfer molding (RTM)—to produce thinner laminates when required.

The finite element results closely matched the experimental data, confirming the accuracy of the numerical model and the reliability of the coupled-field analysis method. The Schapery-based rule of mixtures provided satisfactory predictions for thermal expansion coefficients in isotropic-type composites and yielded good correlation with experimental results for critical buckling temperatures.

REFERERENCES

[1] Eruslu, S.O., Akyol, U., Agirgan, A.O.& Taskin, E. (2015). Farklı takviye malzemeleriyle desteklenmiş plastik esaslı hibrid kompozit malzemelerde termal şekil değiştirme ve burkulma davranışının incelenmesi. (Bap Proje No: NKUBAP.00.17.AR.12.06).

[2] Shivakumar, K. N. , Sundaresan, M. J. & Avva, V. S. (1999). Structural integrity of discontinuous stiffened ıntegrally braided and woven composite panels, 38th Structures, Structural Dynamics, and Materials Conference. AIAA Conference Proceedings.

[3] Yoshino,T.& Ohtsuka,T.(1982).Inner stress analysis of plane woven fiber reinforced plastic laminates.Bulletin of the JSME,25(202),485-492.

[4] Ishikawa,T.& Chou, T.-W. (1982). Elastic behavior of woven hybrid composites,Journal of Composite Materials,16(1),2-19.

[5] Bozkurt E., Kaya E.& Tanoglu M. (2007). Mechanical and thermal behavior of non-crimp glass fiber-reinforced layered clay/epoxy nanocomposites, Composite Science and Tech., 67(15–16), 3394–3403.

[6] Drapier, S. &Wisnom M.R.(1999). Finite-element investigation of the compressive strength of non-crimp-fabric-based composites. Composites Science and Technology. 59(8),1287-1297.

[7] Schapery R.A.,(1968), Thermal expansion coefficients of composite materials based on energy principles**.** Journal of Composite Materials, 2(3), 380-404.

[8] Ishikawa,T.& Chou, T.-W. (1983). In-plane thermal expansion and thermal bending coefficients of fabric composites.Journal of Composite Materials,17(2),92-104.

[9] Chamberlain, N.J. (1968). Derivation of Expansion Coefficients for a Fibre Reinforced Composites. Report 33, British Aircraft Corporation: London, UK.

[10] Rogers, K.F.,Phillips, L.N., Kingston-Lee, D.M., Yates, B., Overy M.J.& Sargent, J.P., (1977). The Thermal Expansion of Carbon Fibre-Reinforced Plastics. Journal of Materials Science, 12, 718-734.

[11] Hsu Y.S., Reddy J.N.& Bert C.W. (1981). Thermoelasticity of circular cylindirical shells laminated of bimodulus composite materials. Journal of Thermal Stresses 4(2),155-177.

[12] Reddy J.N.& Hsu Y.S. (1980). Effects of shear deformation and anisotropy on the thermal bending of layered composite plates. Journal of Thermal Stresses 3(4), 475-493.

[13] Reddy J.N.& Chao W.C., (1981), Non-linear bending of thick rectangular, laminated composite plates, International Journal of Non-Linear Mechanics,16 (3-4), 291–301.

[14] Kant,T.& Babu, C. S. (2000). Thermal buckling analysis of skew fibre-reinforced composite and sandwich plates using shear deformable finite element models. Composite Structures, 49 (1), 77–85.

[15] Jones R.M. (2005).Thermal buckling of uniformly heated unidirectional and symmetric cross-ply laminated fiber-reinforced composite uniaxial in-plane restrained simply supported rectangular plates, Composites Part A: Applied science and manufacturing. 36(10), 1355–1367.

[16] Aydogdu M. (2007). Thermal buckling analysis of cross-ply laminated composite beams with general boundary conditions , Composites Science and Technology, 67 ,1096–1104.

[17] Pradeep, V. & Ganesan,N.(2008). Thermal buckling and vibration behavior of multi-layer rectangular viscoelastic sandwich plates. Journal of Sound and Vibration,310 (1-2),169-183.

[18] Matsunaga H., (2006). Thermal buckling of angle-ply laminated composite and sandwich plates according to a global higher-order deformation theory, Composite Structures,72(2), 177–192.

[19] Mikhasev,G.I.& Altenbach, H. (2019). Thin-walled laminated structures buckling, vibrations and their suppression.Advanced Structured Materials, Springer.

[20] Ahmed, O.S., Aabid, A., Muhammed Ali, J.S., Hrairi,M.& Yatim,N.M. (2023). Progresses and challenges of composite laminates in thin-walled structures: a systematic review.ACS Omega,8,30824-30837.

[21] Ahmed, O.S., Muhammed Ali, J.S., Aabid, A., Hrairi, M., & Yatim, N.M. (2024). Parametric analysis of critical buckling in composite laminate structures under mechanical and thermal loads: a finite element and machine learning approach. Materials,17(17),4367.

[22] Deng, W.-L., Wang, B.-W., Lei, K.& Wu,J.-T.(2023).Thermal buckling behavior of metal/composite wall panels.Journal of Physics: Conference Series The 13th Asia Conference on Mechanical and Aerospace Engineering,2472(1).

[23] Eruslu S.Ö., Aydogdu M.,Filiz S.,(2012) ,Thermal buckling analysis of short fiber reinforced laminated plates, Mechanics of Nano, Micro and Macro Composite Structures Conference.

[24] Baran,F.,Balkan,D.(2023). Thermal buckling analysis of laminated plates with variable angle fiber orientation, NÖHÜ Müh. Bilim. Derg.,12(3),912-918. Graduate School of Science and Technology.

[25] Mercan,E. (2023). Thermal buckling of laminated plates wıth variable fıber volume fraction (Master of Science Thesis). Middle East Technical University, The Graduate School of Natural and Applied Sciences

[26] Eruslu S.Ö. (2008). Kısa Elyaf Takviyeli Kompozit Plaklarda Titreşim Analizi (Doctoral Thesis). Trakya University, Mechanical Engineering, The Graduate School of Natural and Applied Sciences

[27] Taskin,E.(2015). Kevlar/karbon elyaf takviyeli lamina kompozitlerde termal şekil değiştirme davranışının incelenmesi, (Master of Science Thesis), Namık Kemal

University, Mechanical Engineering, The Graduate School of Natural and Applied Sciences.

[28] University of Twente Technical Report. (1999), Theoretical background I Woven fabric composite properties. https://www.utwente.nl/en/et/ms3/research-chairs/pt/Tools/Files/U20MM%20background%20information.pdf

[29] Eruslu, S.O., Agırgan, A.O., Taskin,E.(2014). Thermal stability and residual effects on carbon kevlar fabric composites [Conference poster]. 6th International İstanbul Conference on Future Technical Textile FTT.

CHAPTER 3

THE EFFECT OF COOLING PHOTOVOLTAIC (PV) PANELS ON ELECTRICAL POWER GENERATION

İsmail KARALI[1]

1 Dr. Instructor, Gaziantep University, Technical Sciences Vocational School, Department of Electricity and Energy, Gaziantep, Türkiye, ORCID ID: 0000-0002-3520-456X E-mail: ismailkarali@gantep.edu.tr

1. Introduction

The rapid growth of the world population and the accelerating pace of industrialization have led to a continuous rise in global energy demand, while existing energy resources have become increasingly inadequate to meet this demand. It is estimated that global energy consumption will reach twice the 1998 level by 2035 and triple by 2055 [1]. This dramatic increase places energy supply, energy security, and environmental sustainability at the center of the international agenda. Conventional and limited fossil resources—such as oil, natural gas, coal, lignite, and nuclear energy—generate high carbon emissions, resulting in serious environmental problems including global warming, air pollution, and ecological degradation [2]. The intensive use of these resources in residential areas, transportation, and industry further complicates their environmental impacts and underscores the urgency of adopting sustainable energy approaches.

Renewable energy refers to energy sources that are naturally replenished and inexhaustible, and it plays a critical role in the global energy transition due to its low environmental footprint [3]. International energy authorities project that the share of renewable energy in total global energy production will reach approximately 45% in the coming years [4]. Furthermore, by 2050, the largest growth among renewable resources is expected to occur in solar energy [5]. In this context, increasing the role of solar energy in long-term national energy strategies has become both an economic and environmental necessity.

Photovoltaic (PV) panels are among the most widely used technological solutions for converting solar energy directly into electrical energy. The electrical efficiency of PV panels depends on several parameters, including module material, solar irradiance, ambient temperature, and particularly module temperature [6]. The literature reports that the adverse effect of temperature elevation on PV efficiency is highly pronounced [7]. In many geographical regions, high ambient temperatures cause PV module temperatures to rise significantly above the surrounding air temperature during daylight hours. This temperature rise reduces panel efficiency through physical mechanisms such as bandgap narrowing and changes in carrier recombination rates. The black-surfaced cell design further intensifies this issue by absorbing a large portion of solar energy as heat, leading to even higher temperature increases [8]. Experimental studies have demonstrated that PV surface temperatures can reach up to 80 °C, resulting in efficiency losses of up to 8% [9]. These findings clearly highlight that temperature regulation is a critical determinant of energy production performance in PV systems.

Accordingly, various passive and active cooling techniques have been developed to limit temperature increases in PV panels. Among these, passive cooling methods are particularly attractive for commercial applications because they require no additional energy input and do not increase system cost [10]. In this study, the effectiveness of passive cooling methods aimed at reducing PV panel temperature and enhancing electrical efficiency is investigated. Two different passive cooling configurations—comprising heat pipes and finned heat sinks—were integrated into PV panels, and their performance outcomes were comparatively analyzed. In doing so, the study provides innovative and practically oriented findings that contribute to the existing literature on PV cooling technologies.

2. Photovoltaic Cells

2.1. Cell Structure and Material Types

Photovoltaic (PV) cells are semiconductor devices that convert incident solar energy (photons) directly into electrical energy, and they are commonly referred to in the literature as solar cells or photovoltaic panels. PV cells can be manufactured in various geometrical shapes, with square, rectangular, and circular designs being the most widely used. A typical solar cell has an active surface area of approximately 100 cm², while its thickness ranges between 0.2 and 0.4 mm depending on the fabrication technology. The conversion efficiency of PV cells can reach up to approximately 25%, depending on the semiconductor material used—such as mono-Si, poly-Si, or thin-film technologies—and the associated manufacturing processes [11]. This efficiency range highlights the critical influence of advances in materials science and production technologies on PV performance.

As illustrated in Figure 1, solar cells can be interconnected in series or parallel to enhance their power generation capability. When combined in this manner, the resulting assembly is referred to as a photovoltaic panel or solar module. Depending on the required power output, series connections provide higher voltage, while parallel connections allow higher current production. Through such configurations, PV systems with a wide range of power levels can be designed to meet specific application requirements. Therefore, the proper selection of cell and module configuration is a decisive parameter in ensuring both the efficiency and operational performance of photovoltaic systems.

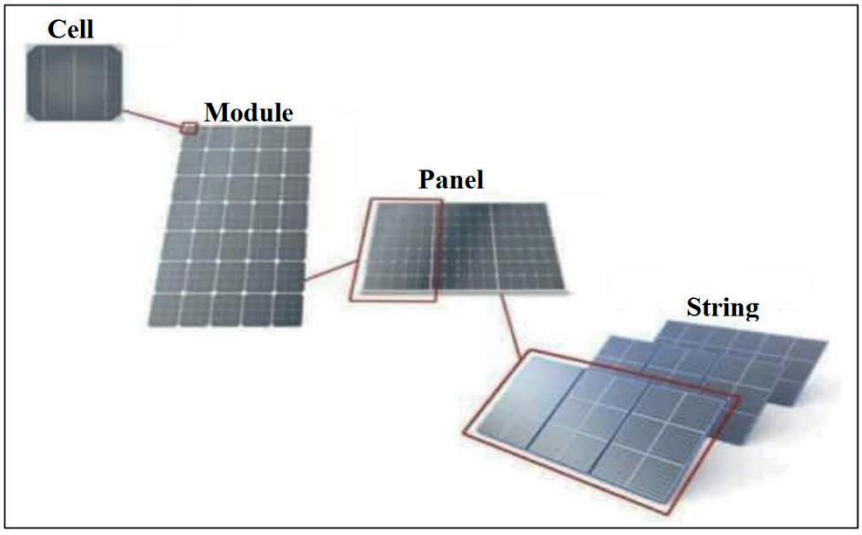

Figure 1. PV Panel Structures.

2.2. Operating Principle of Solar Cells

Solar cells are manufactured from semiconductor materials commonly used in electronic components such as transistors and diodes. Although a variety of semiconductors can be utilized for photovoltaic applications, gallium arsenide (GaAs), silicon (Si), and cadmium telluride (CdTe) are among the most widely preferred materials. The semiconductor properties of these materials constitute the fundamental physical basis of photovoltaic energy conversion.

For a semiconductor to be used in solar cell fabrication, it must be doped as either N-type or P-type. Doping refers to the introduction of a controlled amount of impurity atoms into

the molten intrinsic semiconductor. The position of the dopant in the periodic table determines the resulting semiconductor type.

To produce N-type silicon—the most widely used semiconductor in PV technology—an element from Group V, such as phosphorus, is added. Because phosphorus has five valence electrons whereas silicon has four, the extra electron becomes a free carrier within the crystal structure. For this reason, Group V elements are referred to as "donors" or "N-type dopants." Conversely, P-type semiconductors are produced by adding a Group III element, such as aluminum, into the silicon melt. These trivalent atoms create electron deficiencies in the crystal lattice, forming positively charged carriers known as "holes." Thus, Group III elements are called "acceptors" or "P-type dopants."

When N-type and P-type materials are joined together, a P–N junction is formed. Before junction formation, each region is electrically neutral: electrons are the majority carriers in the N region, while holes dominate in the P region. Upon contact, electrons diffuse from the N to the P side, whereas holes migrate in the opposite direction. This bidirectional diffusion results in a charge redistribution that forms the depletion region. The accumulated charge separation creates a built-in electric field, which plays a key role in photovoltaic energy conversion.

Photovoltaic conversion takes place predominantly within the P–N junction region and progresses through two fundamental steps:

(i) absorption of photons that generate electron–hole pairs in the semiconductor,
(ii) separation and transport of these carriers by the built-in electric field of the depletion region (Kincay et al., 2012).

Electrons and holes separated by this electric field accumulate at opposite terminals, resulting in a potential difference and enabling current flow through the external circuit. In this way, solar radiation is directly converted into electrical energy.

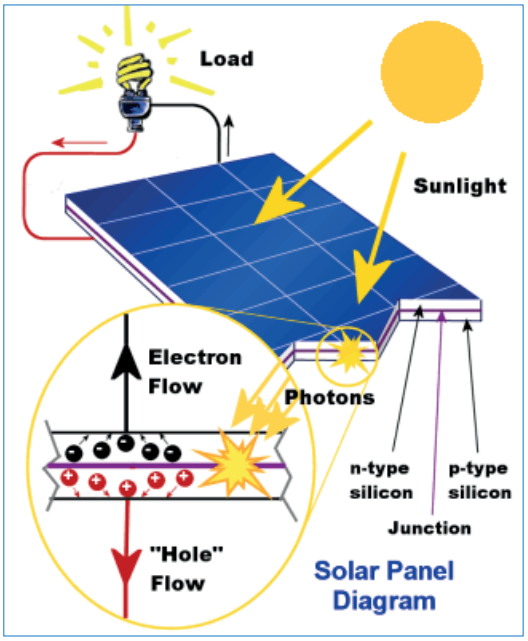

Figure 2. Basic operational mechanism of photovoltaic solar cells.

The electrical current generated by a PV panel is directly related to the incident irradiance. As irradiance increases, the number of photons rises, thereby increasing the photocurrent. Due to their semiconductor nature, PV cells exhibit diode-like electrical behavior; hence, their output characteristics are significantly influenced by both irradiance intensity and cell temperature. Series resistances formed within the junction cause carrier transport losses and constitute one of the key parameters limiting cell efficiency.

The output power of a solar cell reaches its maximum at a specific voltage–current pair known as the maximum power point (MPP). The location of the MPP varies with the photon flux (irradiance) and module temperature. Therefore, operating PV panels at the MPP is crucial for achieving high conversion efficiency [12]. Continuous tracking and regulation of the MPP are essential in industrial PV systems to ensure sustainable and optimal energy production.

3. Material and Method

In this study, the aim is to reduce the excessive heating that leads to efficiency losses in photovoltaic (PV) panels and thereby improve the overall panel performance. Two different passive cooling approaches were evaluated during the experimental stage:

- ✓ The system employing heat pipes together with a flat aluminum heat-absorbing plate (PV-HP),
- ✓ The system utilizing an aluminum finned heat-sink structure (PV-AF).

These cooling arrangements were selected due to their low cost, the availability of commercially accessible components, and their ease of installation and integration. The effectiveness of passive cooling solutions—particularly in systems with low power demand and minimal maintenance requirements—is widely emphasized in the literature, supporting the applicability of the designs selected in this study.

Three monocrystalline photovoltaic panels were used in the experimental setup, and their technical specifications are presented in Table 1. To enable a performance comparison between the PV-HP and PV-AF systems, a non-cooled PV panel was also included as a reference. Thus, the effects of cooling on panel temperature and power generation could be directly evaluated.

Table 1. Technical specifications of the photovoltaic panel

Parameters	**Symbol**	**Values**	**Unit**
Maximum power	Pmax	50	W
Power tolerance	—	±5	%
Open-circuit voltage	Voc	24.62	V
Short-circuit current	Isc	2.57	A
Maximum power voltage	Vmp	20.84	V
Maximum power current	Imp	2.46	A

Previous studies indicate that the optimum tilt angle for photovoltaic systems in the Gaziantep region is approximately 30°. Therefore, a specially manufactured support frame with a 30° tilt angle was used throughout the experimental process to ensure that all panels were tested under identical conditions. As shown in Figure 3, the experimental setup was mounted on this frame.

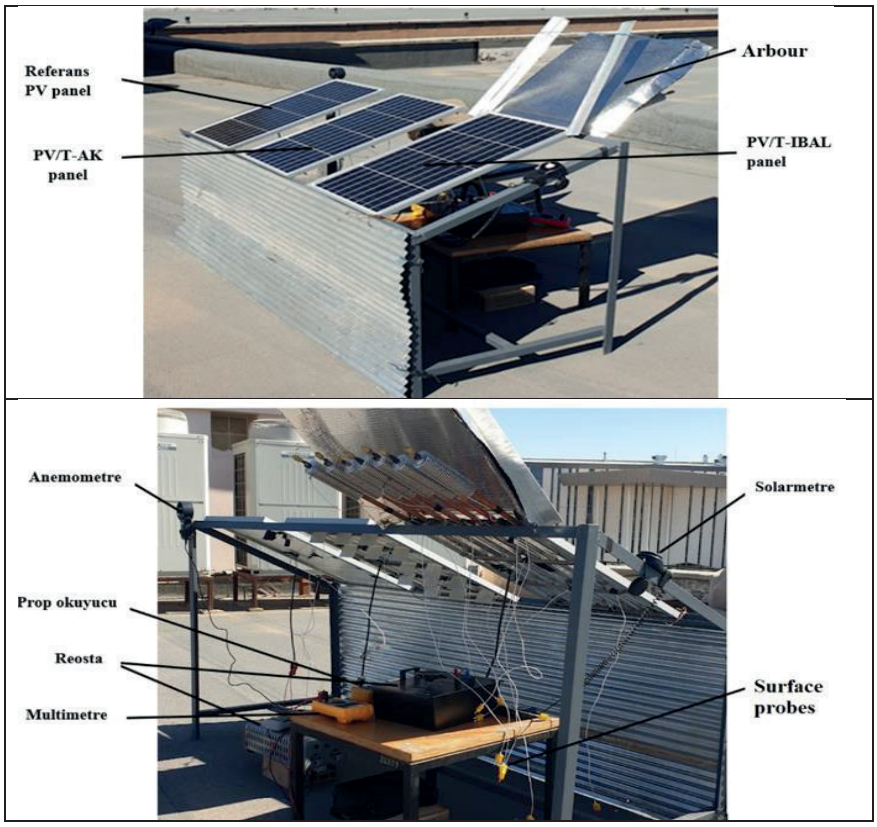

Figure 3. Experimental setup.

A schematic representation of the experimental configuration is provided in Figure 4. These illustrations offer explanatory details regarding the geometric structure of the applied cooling solutions, their contact areas with the panel surfaces, and the associated heat-transfer pathways.

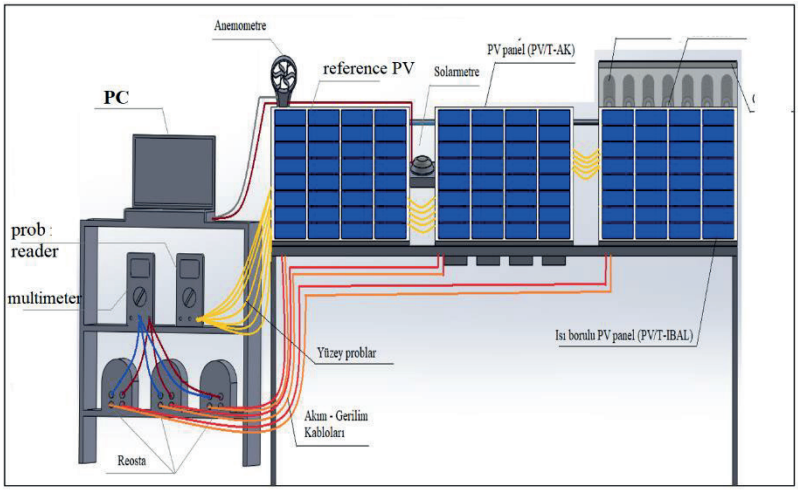

Figure 4. Schematic representation of the experimental setup [3].

3.1. Measurement Devices and Technical Specifications

During the experimental study, the primary parameters influencing the thermal and electrical performance of photovoltaic panels were measured in detail. These parameters include panel surface temperature, ambient temperature, wind speed, solar radiation, evaporator and condenser temperatures of the heat pipes, load current (Imp), load voltage (Vmp), short-

circuit current (Isc), and open-circuit voltage (Voc). Since the literature emphasizes that panel temperature, irradiation intensity, and electrical characteristics are the key variables determining PV performance [13], ensuring high accuracy in recording these parameters was considered a fundamental priority throughout the experiments.

Panel surface temperatures and ambient temperature were measured using LYK 389 model K-type air and surface probes. These probes allow temperature measurements within the range of –50 to +350 °C, enabling precise monitoring of the daily temperature variations of the PV panels. Considering that panel temperature decreases cell efficiency linearly (approximately –0.4 to –0.5%/°C), the accuracy of temperature measurements is critically important for the reliable interpretation of system performance results. For data validation, a Benetech GM320 infrared thermometer was additionally employed, allowing comparison between contact and non-contact measurement techniques and thus enhancing overall measurement reliability. All temperature measurement devices used in the experiment are shown in Figure 5.

Figure 5. Surface probe (thermocouple), (b) probe reader, and (c) infrared thermometer.

Wind speed, which is one of the mandatory parameters in thermodynamic analyses, was measured using a CEM-DT-619 anemometer. With a measurement range of 0.4–30 m/s and an accuracy of ±3% or ±0.20 m/s, this device provides sufficient precision for evaluating the cooling effect of natural convection on the panel surface. Since previous studies have shown that increases in wind speed reduce PV panel surface temperature and thereby enhance output power [14], recording this parameter is essential for maintaining the analytical integrity of the study.

The electrical performance of the photovoltaic panels was determined using current and voltage data measured with a Fluke 15B+ digital multimeter. The device is capable of measuring up to 1000 V in DC/AC voltage and 10 A / 400 µA in current, and its ±0.5% basic DC accuracy enables reliable extraction of PV characteristic curves. The accuracy of electrical measurements is particularly critical for determining the maximum power point (MPP), which is a key metric in PV performance evaluation.

Solar irradiance was measured using a CEM DT-1307 solar meter, which can measure up to 1999 W/m² with an accuracy of ±10 W/m². This level of precision lies within the widely accepted limits for experimental PV studies. Since instantaneous variations in solar radiation directly influence PV output power, irradiance data significantly enhanced the reliability of performance comparisons.

During the experimental period, a variable resistor with a capacity of 5 A and 15 Ω was used to ensure a consistent load on the panels. This approach allowed all PV panels to be tested under comparable loading conditions during each measurement interval, thereby improving the consistency of inter-system comparisons. The measurement devices used in the study are presented in Figure 6.

Figure 6. (a) Anemometer, (b) solar meter, and (c) rheostat.

4. Results and Discussion

Solar energy is one of the most significant renewable energy resources today due to its sustainability and broad accessibility [15]. Even under cloudy weather conditions, where solar irradiance decreases because of seasonal and meteorological variations, electricity generation can still be achieved, which is primarily the result of advances in photovoltaic (PV) technologies [16]. This capability enables PV systems to operate not only under high irradiance conditions but also at low irradiance levels, thereby expanding the utilization of solar energy across a wide range of applications, including heating, cooling, and electricity generation.

PV panels, which directly convert solar energy into electrical power, have become central components of modern energy-generation technologies. Although PV manufacturing costs were considerably high in the past, current production technologies have significantly reduced these costs, placing PV panels among the most economically viable methods of electricity generation [17]. Nevertheless, commercial PV modules still operate below their theoretical efficiency limits. Among the primary factors that limit PV performance are dust accumulation, shading, surface contamination, and most critically, the increase in cell temperature. Temperature rise reduces the semiconductor bandgap, leading to a decrease in the output voltage, which in turn causes noticeable performance losses. Previous studies have shown that each 1 °C increase in cell temperature can reduce panel efficiency by approximately 0.4–0.5% [18].

The present work aims to mitigate efficiency losses caused by temperature increases in PV panels and investigates the potential for reducing panel temperatures using passive cooling methods. Passive cooling solutions are gaining increasing attention in the literature due to their simplicity and the fact that they do not require additional power consumption. In the experimental analysis, improvements in performance resulting from controlled panel surface temperatures were comprehensively evaluated. The temperature–power relationship of the PV module, the effectiveness of passive cooling systems, and comparative performance differences with the reference (non-cooled) panel were analyzed. The findings obtained in this study align with existing literature and further support the applicability and performance benefits of passive cooling approaches in PV systems.

4.1. Experimental Results

In this study, the performance of two different passive cooling methods was evaluated with the aim of reducing efficiency losses associated with increased cell temperature in photovoltaic panels. The experimentally investigated systems were the PV-HP

configuration, which integrates heat pipes with a flat aluminum heat-absorbing plate, and the PV-AF configuration, which utilizes an array of aluminum cooling fins. Both cooling structures require no additional power consumption, are cost-effective, consist of easily accessible components, and offer practical applicability. Therefore, they align well with passive cooling strategies widely recommended in the literature. In this context, the study supports the commonly emphasized approach that "simple yet effective passive cooling mechanisms can be readily integrated into field applications."

Before commencing the experimental procedures, the functional accuracy of the PV panels was tested, and their compatibility with nominal specifications was confirmed. This step ensured that the influence of the cooling systems on panel performance could be assessed in an isolated and controlled manner. The experiments were conducted outdoors in Gaziantep, Türkiye, an area located at the intersection of Mediterranean and continental climate zones, during September and between 10:00 and 18:00. Throughout the experimental period, ambient temperature ranged from 30 to 37 °C, solar irradiance varied between 179 and 1,077 W/m², and wind speed fluctuated between 0.34 and 2.15 m/s. These meteorological parameters directly affect PV panel performance and were therefore continuously recorded.

During the experiments, ambient temperature, solar irradiance, wind speed, average surface temperatures of the PV panels, and electrical output power were monitored. Since rapid changes in wind speed or irradiance due to cloud movement can influence measurement stability under open-field conditions, experiments were repeated on different days to enhance data reliability. Time-averaged values from repeated measurements were used in the analysis. This methodological approach is consistent with recommendations in field-based experimental PV studies and increases the statistical significance of the results.

Based on the recorded data, energy and performance analyses were conducted, and the temperature–power characteristics of the PV-HP, PV-AF, and non-cooled reference panel were comparatively examined. These analyses clearly demonstrate the effectiveness of passive cooling methods in mitigating temperature-induced efficiency losses in PV panels, and the observed trends are consistent with similar findings reported in the literature.

4.2. Comparison of Surface Temperatures and Electrical Power Outputs of Photovoltaic Panels

In this study, two passive cooling systems designed to mitigate temperature-induced performance losses in photovoltaic panels were investigated. The first system is the PV-HP configuration, which integrates a heat pipe with an aluminum flat plate heat sink, and the second is the PV-AF configuration, which utilizes aluminum finned heat sinks. The surface temperatures, temperature differentials, power outputs, and electrical efficiencies of the cooled panels were comparatively evaluated.

According to the data presented in Figure 7, the minimum–maximum surface temperatures of the PV-HP, PV-AF, and the uncooled reference panel were measured as 34–45 °C, 42–51 °C, and 45–54 °C, respectively. The daily average panel temperatures were obtained as 39.7 °C for PV-HP, 44.6 °C for PV-AF, and 47.7 °C for the reference panel. These results indicate that the PV-HP system operated approximately 8 °C cooler than the reference panel, while the PV-AF system operated about 3 °C cooler. Furthermore, the PV-HP system achieved surface temperatures approximately 5 °C lower than those of the PV-AF system. The reduction in temperature differences after 17:00, as solar irradiance decreases, is consistent with literature reports indicating the diminished effectiveness of passive cooling systems during the late afternoon.

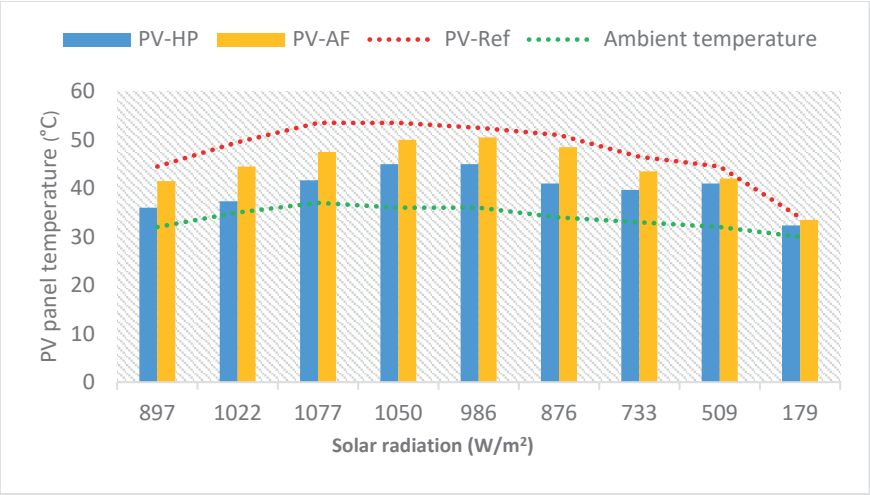

Figure 7. PV panel temperatures as a function of solar irradiance.

Analysis of the electrical power outputs shows that the minimum–maximum power values for the PV-HP panel were 9.46–47.09 W, with an average of 36.19 W. For the PV-AF panel, the values ranged between 8.75–46.70 W, with an average power of 35.67 W. The uncooled reference panel produced 7.59–46.18 W, with an average output of 34.83 W.

Based on these findings, the PV-HP and PV-AF systems provided 5.13% and 2.56% higher electrical efficiency compared to the reference panel, respectively. Moreover, the PV-HP system exhibited an approximately 2.50% efficiency advantage over the PV-AF system. This improvement can be attributed to the effective heat transfer capability of the heat pipes in the PV-HP configuration, which maintains a more stable and lower panel surface temperature. Similar trends are widely reported in the literature, indicating that heat-pipe-based passive cooling systems enhance panel efficiency particularly under moderate-to-high irradiance conditions.

The variation of power enhancement with respect to solar irradiance and ambient temperature is presented in detail in Figure 8. This graph clearly demonstrates the inverse relationship between panel temperature and electrical output, providing field-measured evidence of the effectiveness of passive cooling methods.

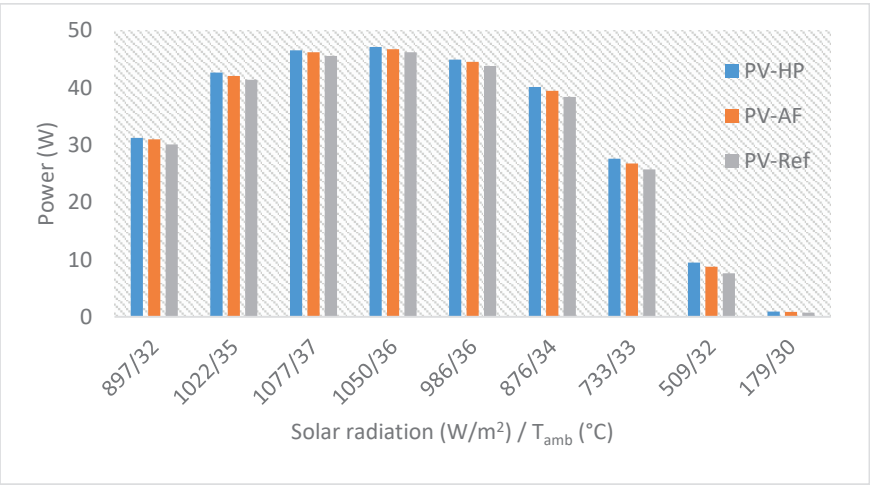

Figure 8. PV panel power output as a function of solar irradiance and ambient temperature.

4.3. Effect of Temperature and Wind Speed on the Efficiency of Photovoltaic Panels

The instantaneous efficiencies of photovoltaic (PV) panels vary depending on the semiconductor material properties of the module, the intensity of incoming solar irradiance, the ambient temperature, and directly on the module surface temperature. According to widely accepted findings in the literature, each 1 °C increase in PV module temperature results in approximately 0.4–0.5% loss in electrical efficiency. Therefore, controlling the panel surface temperature is considered a critical parameter for improving PV system performance, particularly in hot climatic regions.

The experimental data obtained in this study reveal a clear linear relationship between the electrical power generated by the panel and the solar irradiance intensity, as shown in Figure 8. However, while increasing irradiance enhances power generation, it also raises the panel temperature, creating a dual–direction effect on overall efficiency. Hence, when evaluating cooling techniques aimed at improving panel efficiency, not only irradiance but also environmental variables such as ambient temperature and wind speed must be considered.

In this context, the effect of wind speed on panel temperatures was separately analyzed, and the variations in module temperature are presented in Figure 9. The measurements indicate that wind speed exhibits sudden fluctuations due to cloud movements, variations in wind direction, and local microclimate conditions. For this reason, instead of momentary short-scale data, hourly averaged wind speeds—which provide more stable trends—were used in the assessment.

The influence of wind speed was examined in two time intervals: before and after 12:30. The average solar irradiance intensities for these periods were determined as 999 W/m² and 971 W/m², respectively. Similarly, the average wind speeds were recorded as 0.79 m/s and 0.93 m/s. Thus, despite a 2.8% decrease in irradiance, an approximately 17.7% increase in wind speed resulted in an ~8.5% increase in power output for the PV-HP, PV-AF, and reference panels.

This finding is consistent with studies in the literature emphasizing the role of wind-driven natural convection in enhancing PV cooling performance. It has been widely reported that even small increments in wind speed can significantly reduce module temperature and consequently lead to notable improvements in PV efficiency, particularly in hot climatic conditions. Similarly, the present study demonstrates that environmental wind speed acts as a complementary factor that enhances the effectiveness of passive cooling systems.

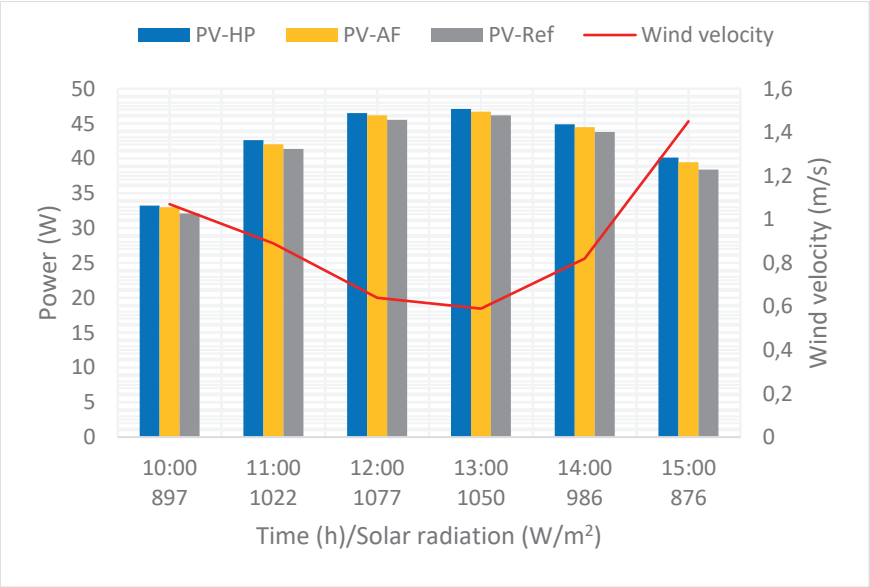

Figure 9. Effect of wind velocity on the power production of PV panels.

4.4. Energy Analysis of PV Systems and Comparison of Electrical Efficiencies

A detailed energy analysis was carried out to reveal the comparative performance of the photovoltaic panels used in the experiment. In this analysis, thermal and electrical efficiencies, maximum power values, time-dependent variations of solar irradiance, and environmental conditions such as wind speed were evaluated together. Thus, the holistic effect of passive cooling methods on panel behavior was determined.

The electrical efficiency of the reference PV panel ranged between 1.41% and 15.48% depending on the changes in irradiance and module temperature throughout the day, and the average efficiency was calculated as 11.7%. This result indicates that the reference panel experiences significant efficiency losses particularly during periods of high irradiance and high temperature. The large number of studies in the literature explaining the negative effect of PV module temperature on efficiency confirms that these findings are consistent with expected trends.

In the PV-HP system, which uses heat pipes together with an aluminum flat heat sink, the measured electrical efficiency ranged between 1.77% and 15.96%, with an average efficiency of 12.3%. This corresponds to an improvement of approximately 5.13% compared with the reference panel. The increase in the PV-HP panel is attributed to the effective removal of heat from the back surface of the panel due to the high thermal conductivity of heat pipes, which significantly reduces the module temperature. This observation is consistent with the efficiency improvements frequently reported in the literature for passive heat-pipe-based systems.

For the PV-AF panel cooled with aluminum fins, the efficiency ranged from 1.65% to 15.75%, with an average value of 12.0%. This corresponds to an improvement of approximately 2.56% compared with the reference panel. The improvement in the PV-AF system is associated with enhanced natural convective heat transfer enabled by the fins. However, since the heat-pipe design provides more effective heat removal, the PV-HP system achieved higher efficiency than PV-AF.

Both passive cooling methods were experimentally found to have positive effects on electrical efficiency. However, the cooling effectiveness was more pronounced in the PV-HP system, resulting in higher efficiency improvement. This is attributed to the high heat

transport capacity of heat pipes and their ability to homogenize heat distribution, which reduces maximum peak surface temperatures on the panel.

The irradiance levels and time-dependent electrical efficiencies of the panels used in the experiment are presented in Figure 10, demonstrating that passive cooling methods provide more noticeable efficiency improvements, especially during high-irradiance periods.

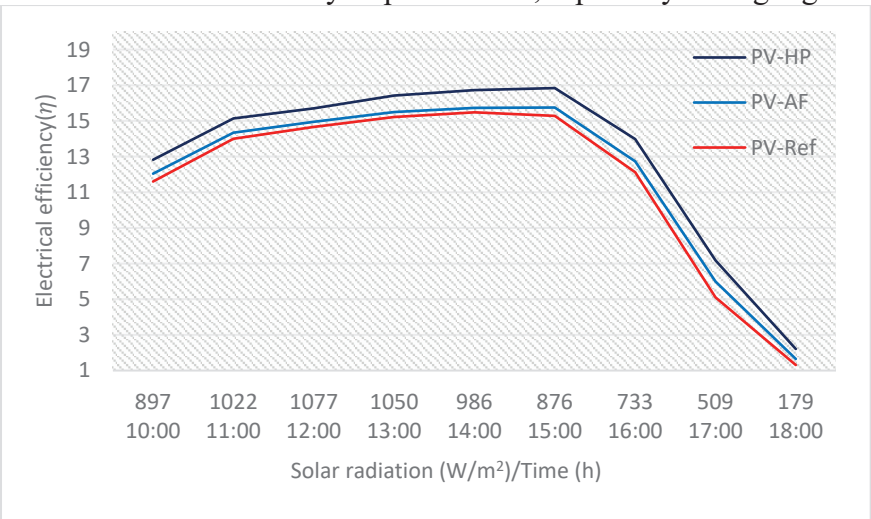

Figure 10. Electrical efficiency as a function of solar irradiance.

5. Conclusion

This study experimentally investigated the performance of two passive cooling approaches—heat pipe–assisted configuration (PV-HP) and fin-enhanced aluminum heat sink configuration (PV-AF)—implemented to mitigate temperature-induced efficiency losses in photovoltaic (PV) panels. The performance of these systems was comparatively evaluated against an uncooled reference PV panel. The experimental data and revised calculations demonstrate that both improved cooling configurations effectively reduce the panel surface temperature and consequently enhance the electrical performance.

According to the corrected results, the PV-HP system achieved approximately 5.13% higher electrical efficiency compared to the reference panel, whereas the PV-AF configuration provided an improvement of about 2.56%. These enhancements are directly associated with the reduction in module temperature, as the literature consistently reports that each 1 °C increase in PV module temperature decreases electrical efficiency by approximately 0.3–0.5%. Therefore, the observed efficiency gains align well with the thermophysical mechanisms governing PV performance.

Throughout the experimental period, the observed increase in wind speed also contributed to cooling performance. While the baseline average wind velocity was 0.79 m/s, the measured value reached 0.93 m/s, corresponding to an increase of roughly 17.7%. This rise strengthened the natural convection process and further supported the effectiveness of passive cooling. Such findings are consistent with previous studies emphasizing the significance of ambient wind effects in natural-convection-based PV cooling systems.

Overall, the results clearly indicate that both the heat-pipe-assisted and fin-enhanced passive cooling configurations improve the thermal behavior of PV modules and yield meaningful enhancements in electrical output. However, the PV-HP configuration outperformed the PV-AF system, primarily due to its superior thermal conductivity and more effective heat spreading capability.

These findings confirm that passive cooling techniques constitute a practical and sustainable option for enhancing PV system performance owing to their low cost,

maintenance-free operation, and ease of integration. Future studies are recommended to examine the behavior of these passive structures under different climatic conditions, develop optimization models, and evaluate hybrid (active + passive) cooling solutions.

6. References

[1] S. Y. Özkaya, "Yenilenebilir Enerji Kaynakları," T.C. Dışişleri Bakanlığı, 2025. [Online]. Available: https://www.mfa.gov.tr/yenilenebilir-enerji-kaynaklari.tr.mfa (accessed Feb. 19, 2025).

[2] International Energy Agency (IEA), Renewables 2024: Analysis and Forecast to 2028. Paris: IEA, 2024. [Online]. Available: https://iea.blob.core.windows.net/assets/17033b62-07a5-4144-8dd0-651cdb6caa24/Renewables2024.pdf(accessed Feb. 19, 2025).

[3] İ. Karali and A. Kabul, "Experimental investigation of using heat pipes and finned heat sink in cooling of PV panels—Thermodynamic and economic analysis consequences," Environmental Progress & Sustainable Energy, vol. –, pp. e70133, 2025. doi: 10.1002/ep.70133.

[4] European Commission, "Renewable energy targets," 2025. [Online]. Available: https://energy.ec.europa.eu/topics/renewable-energy_en(accessed Aug. 21, 2025).

[5] M. Bayrak and E. Aslan, "Türkiye'deki lisanssız güneş enerjisi santrallerinde üretim kayıplarının belirlenmesi," Kahramanmaraş Sütçü İmam University Journal of Engineering Sciences, vol. 26, no. 1, pp. 233–240, 2023. doi: 10.17780/KSUJES.1210936.

[6] F. Bayrak, H. F. Oztop, and F. Selimefendigil, "Experimental study for the application of different cooling techniques in photovoltaic (PV) panels," Energy Conversion and Management, vol. 212, p. 112789, 2020. doi: 10.1016/j.enconman.2020.112789.

[7] E. Arslan, M. Aktas, and O. F. Can, "Experimental and numerical investigation of a novel photovoltaic thermal (PV/T) collector with the energy and exergy analysis," Journal of Cleaner Production, vol. 276, p. 123255, 2020. doi: 10.1016/j.jclepro.2020.123255.

[8] B. Acar and Ş. Baş, "Investigation of energy generation at test system designed by use of concentrated photovoltaic panel and thermoelectric modules," International Journal of Renewable Energy Research, vol. 8, no. 4, 2018. [Online]. Available: https://www.researchgate.net/publication/330224740.

[9] G. Omeroglu, "Numerical (CFD) and experimental analysis of photovoltaic thermal (PV/T) system," Fırat University Journal of Engineering Sciences, vol. 30, no. 1, pp. 161–167, 2018.

[10] J. Liu, Y. Zhou, Z. Zhou, et al., "Passive photovoltaic cooling: Advances toward low-temperature operation," Advanced Energy Materials, vol. 2, no. 302, p. 662, 2023.

[11] "LONGi launches residential heterojunction back-contact solar module with 25.2% efficiency," PV Magazine International, May 7, 2025. [Online]. Available: https://www.pv-magazine.com/2025/05/07/longi-launches-residential-heterojunction-back-contact-solar-module-with-25-2-efficiency/.

[12] F. Duyan and K. Polat Bayrakdarlar, "Fotovoltaik bir panelin MATLAB Simulink ile modellenmesi ve dış ortam koşullarındaki davranışının incelenmesi," Journal of Architecture and Life, vol. 7, no. 3, pp. 965–980, 2022. doi: 10.26835/my.1197319.

[13] J. A. Duffie and W. A. Beckman, Solar Engineering of Thermal Processes. Hoboken, NJ: Wiley, 2013.

[14] R. Kumar and M. A. Rosen, "A critical review of photovoltaic–thermal solar collectors for air heating," Applied Energy, vol. 88, no. 11, pp. 3603–3614, 2011.

[15] F. Yiğit, İ. Karali, and A. Kabul, "Experimental and ensemble learning-based prediction of heat pipe and aluminum fin cooling effects on PV panel power output for a sustainable future," Thermal Science and Engineering Progress, p. 104067, 2025.

[16] A. F. Almarshoud, M. A. Abdel-Halim, R. A. Almasri, and A. M. Alshwairekh, “Exergy and energy analysis of bifacial PV module performance on a cloudy day in Saudi Arabia,” Sustainability, vol. 16, no. 17, p. 7428, 2024. doi: 10.3390/su16177428.
[17] X. Liu, E. Fernandez, and C. Descartes, “Global PV supply chains: Costs and energy savings, GHG emission reductions,” Renewable Energy Journal, preprint, Research Square, May 25, 2023. doi: 10.21203/rs.3.rs-2979030/v1.
[18] Y. Liu, Y. Chen, D. Wang, et al., “Experimental and numerical analyses of parameter optimization of photovoltaic cooling system,” Energy, vol. 215, p. 119159, 2021. doi: 10.1016/j.energy.2020.119159.